β-Glucan Transferases of Family GH17 from Proteobacteria

Jón Óskar Jónsson Wheat

Líffræðideild
Háskóli Íslands
2010

β-Glucan Transferases of family GH17 from Proteobacteria

Jón Óskar Jónsson Wheat

90 eininga ritgerð sem er hluti af
Magister Scientiarum gráðu í Líffræði

Leiðbeinendur
Guðmundur Óli Hreggviðsson
Ólafur Héðinn Friðjónsson

Prófdómari
Jón Magnús Einarsson

Líf-og umhverfisfræðideild
Verkfræði- og náttúruvísindasvið
Háskóli Íslands

Divison of Biomolecules and Biotechnology
Matis ehf.

Reykjavík, Nóvember 2010

β-Glucan Transferases of Family GH17 from Proteobacteria.

90 einninga ritgerð sem er hluti af *Magister Scientiarum* gráðu í Líffræði

Líffræðideild
Verkfræði- og náttúruvísindasvið
Háskóli Íslands
Askja, Sturlugötu 7
107 Reykjavík

Sími: 525 4600

Skráningarupplýsingar:
Jón Óskar Jónsson Wheat, 2010, β-Glucan Transferases , meistararitgerð, Líf- og umhverfisfræðideild, Háskóli Íslands, 57 bls.

Prentun: 01
Reykjavík, Nóvember 2010

Útdráttur

Ensím sem tilheyra fjölskyldu GH17 í flokkunarkerfi sykrurofsensíma voru rannsökuð úr þremur tegundum baktería: *Methylobacillus flagellatus* KT, *Rhodopseudomonas palustris* og *Bradyrhizobium japonicum*. Nýlegar rannsóknir hafa sýnt fram á að slík ensím úr Proteobakteríum sýna transferasa virkni, þ.e. þau klippa β-glúkan fjölsykrur og skeyta bútum á enda þega-sykra með myndun nýrra 1,3 tengja eða mynda greinar með β1,4 eða β1,6 tengjum. Gen ensímanna voru klónuð og tjáð í *E. coli*. Ensímin voru tjáð sem MalE samruna protein, en eftir framleiðslu og hreinsun var MalE hlutinn klipptur af með sérvirkum Ulp1 proteasa. Ensímin voru skilgreind með tilliti til virkni þeirra á laminarin fásykrur. Myndefni voru skilgreind með tilliti til stærðar og tengjagerðar með fjölbreyttri aðferðafræði, TLC, Maldi-TOF, electrospray og NMR. Niðurstöður rannsóknanna leiddu í ljós að tvö þessara ensíma, úr *Rhodopseudomonas palustris* og *Methylobacillus flagellatus* KT mynda β(1-3) tengi og eru því lengingarensím. Ensímið úr *Bradyrhizobium japonicum* sýndi β(1-6) transferasa virkni og er því greinamyndunar-ensím (branching). Unnt var að sýna fram á að ensímið klippir fjölsykrur frá afoxandi enda (reducing end) fjölsykruhvarfefnanna, öfugt við þau bakteríuensím sem hingað til hafa verið rannsökuð. Sá eiginleiki ætti að gera ensíminu úr *Bradyrhizobium japonicum* kleift að búa til fásykruhringi úr β-glúkan fjölsykrum.

Abstract

In this thesis three β-glycosyl transferases which belong to the glycosyl hydrolase family 17 (GH17) are described. The three enzymes studied were from the bacteria: *Methylobacillus flagellatus* KT, *Rhodopseudomonas palustris* and *Bradyrhizobium japonicum*. Recent studies have shown that such enzymes from Proteobacteria have transferase activity, i.e., they cut β-glucan saccharides and transfer a part to β-glucan acceptor molecules by forming a new β(1-3) linkage or by forming branches with β(1-4) or β(1-6) linkages. Genes encoding the enzymes were cloned in *E. coli*. The recombinant enzymes were produced as MalE fusion proteins. After production the Mal E domain was cut off with a specific Ulp1 protease. The enzymes were characterized regarding to their activity on laminarin substrates. Following technology was implemented to study the reaction products: TLC, Maldi-TOF, electrospray and NMR. The results showed that the enzymes from *Rhodopseudomonas palustris* and *Methylobacillus flagellatus* KT formed β(1-3) linkages and are therefore elongation enzymes. The enzyme from *Bradyrhizobium japonicum* showed a β(1-6) transferase activity and is therefore a branching enzyme. The results showed that the enzyme cuts from the reducing end of β-glucan chains, which is different from the enzymes previously described. This property should allow the enzyme from *Bradyrhizobium japonicum* to form cyclic oligosaccharides from β-glucan polysaccharides.

Table of Contents

List of figures

1. Introduction

Glycosyltransferases catalyze the transfer of a glycosylgroup from a high energy donor or oligosaccharide to an acceptor. They can be classified as Leloir or non-Leloir enzymes depending on the type of donor used. The Leloir type of enzymes utilizes nucleotidephosphosugars (NP-sugar-dependent) as donors producing a nucleotide and saccharide as reaction products. The Non-Leloir glycosyltransferases simply transglycosylate between oligosaccharides or polysaccharides transglycosylases and are mechanistically similar to retaining glycosidases (Holden et. al 2003) The best known non-Leloir glycosyltransferases belong to the family GH13, the amylase family. Enzymes in this family act on poly- and/or oligosaccharides consisting of α-1,4 and 1,6 linked glucose units such as starch. This family mainly consists of hydrolases of the retaining kind where the acceptor is a water molecule but important glycosyltransferases in this family include cyclomaltodextrin glucanotransferase (EC 2.4.1.19), branching enzymes or amylo-(1,4-1,6)-transglycosylase (EC 2.4.1.18), and 4-α- glucanotransferase (EC 2.4.1.25). All these enzymes act on starch and starch related oligo- and polysaccharides.

Non-Leloir glucosyltransferases acting on β-glucans are rare. β-glucans are important cell wall components of bacteria, fungi and seaweeds, made up of β(1-3) or β(1-4) glucopyranosyl residues. They can be further classified on the basis of presence/absence of other linkages into various distinct types with different physicochemical properties. Thus laminarin that can be extracted from seaweed has predominantly β(1-3) linkages with β(1-6)-β-side chain branching on every 10th glucose subunit on average. On the other hand β-glucan from barley, oat or wheat have mixed β(1-3) and β(1-4)linkage in the backbone, but no β(1-6) branches, and generally higher molecular weights and viscosities (McIntosh et al., 2005).

The members of the glycosyl hydrolase family GH17 are mostly involved in the hydrolysis of β(1-3)linkages in laminarin and lichenan and act by retaining mechanism. (1-3)(1-6)Glucosyltransferase activity has been described for some of these enzymes originating from fungi: *Aspergillus fumigatus* Bgl2p, *Pichia jading* (in NCBI, yet unpublished); *Candida albicans*; and Bgl2p from *Saccharomyces cerevisae* (Hartland et al, 1996, Hartland et al., 1991, Goldman et al, 1995). The catalytic activity of these enzymes can be described as following a two-step mechanism, similar to glycosyl transferases of family 13, the first step involving the hydrolysis of a β(1-3)linkage of laminarin and related polysaccharides and the second step the formation of a β(1-6)linkage onto a laminarin chain.

In a previous study of the work described here, a number of bacterial putative transglycosylases from glycosyl hydrolase family GH17 were identified in Bacteria (Eubacteria). They had a narrow phylogenetic distribution and were only found in the phylum of Proteobacteria. None of them were characterized on enzymatic level, but two genes encoding such enzymes from *Bradyrhizobium japonicum (ndvB* and *ndvC)* had been shown by mutational analysis to participate in the formation of cyclic β-glucans (Bhagwat et al., 1995). Also, the role of *ndvB* in the biosynthesis of cyclic β(1-3) glucan in *Pseudomonas aeruginosa* was recently demonstrated (Sadovskaya et al. 2010).

This study resulted in production of recombinant bacterial enzymes which were shown to be non-Leloir β-glucan transferases exhibiting besides β(1-3)elongation activity, also β(1-4) or β(1-6)-elongation, or β(1-6)branching activities (see further details in section 1.4) (Hreggvidsson et al. 2010)

Their biological function of these bacterial GH17 enzymes has not been determined, but they are most likely involved in the synthesis of osmoregulated periplasmic glucans (OPGs) similar to the *ndvB* product in *B. japonicum.* OPGs, being common constituents in the envelope of proteobacteria, are necessary for establishing symbiotic relationships between specific plant hosts and bacteria, such as *Agrobacterium tumefaciens* and *Bradyrhizobium japonicum* (Bohin 2000). In other bacteria, such as *Pseudomonas syringae* and *Erwinia chrysanthemi*, they mediate similar plant host interactions but rather as harmful virility factors in disease development (Mukhopadhyay et al. 1988; Talaga et al. 1994; Cogez et al. 2001). Other studies have indicated roles in antibiotic resistance and in formation of biofilms (Lequette et al. 2007; Mah et al. 2003; Sadovskaya et al. 2010).

This thesis describes the cloning and expression of the GH17 domain part of *ndvB* from *Bradyrhizobium japonicum,* which is a two domain protein also including a GH2 domain. Furthermore, characterization of the activity of the GH17 domain is described. In this work, the NdvB GH17 domain was designated Glt20. We also report successful cloning and expression of homologous GH17 domain genes from *Rhodopseudomonas palustris* (*glt13*) and *Methylobacillus flagellates* strain KT *(glt9).* These genes encode enzymes that do not have additional GT2 domains encoded in their genes.

In the following chapters, various studies on GH17 glycosyl transferases will be reviewed. The biological function of the enzymes their products will be discussed and the structure and properties of different β-glucans described. Furthermore, the origin of the enzymes reported in this thesis will be described and the analytical methods to study the structure of β-glucans reviewed.

1.1 Analysis of the primary structure of two domain glycosyl transferases from bacteria

Genes previously identified in Gram negative bacterial species, encoding two domain proteins consisting of an N-terminal GH17 domain and a C-terminal GT2 domain were proposed to be potential structural genes for β-glycosyltransferases or polysaccharide modifying enzymes. One of these genes was *ndvB* from *B. japonicum.* The hydrophobicity profile of deduced amino acid sequences of the *B. japonicum ndvB* encoding enzyme revealed three transmembrane helices between the domains and five transmembrane helices at the far C-terminal end. A putative hydrophobic signal peptide was also identified at the N-terminal side (data not shown). Based on these structural features and the fact that GT2 glycosyltransferases use activated sugar donors, formed in the reduced environment of the cytoplasm, we postulate that the GT2 domain resides on the cytoplasmic side of the bacterial cell membrane and the GH17 domain on the periplasmic side. The transmembrane helices, apart from the N-terminal signal peptide, are predicted to form a membrane pore through which the newly

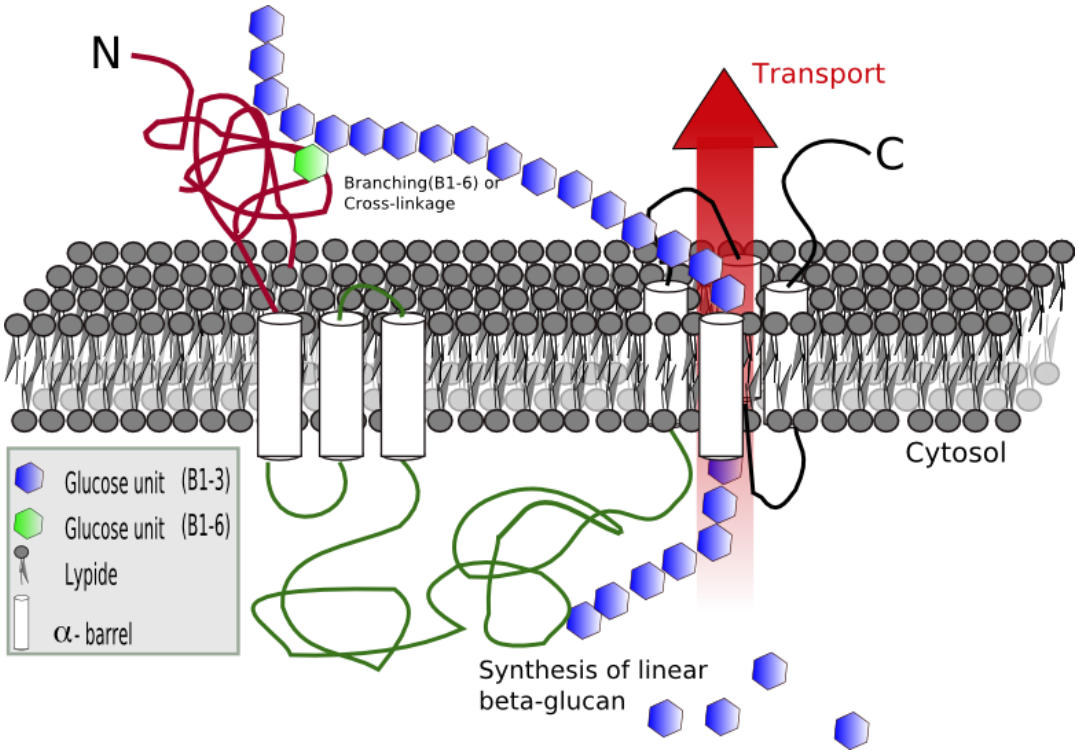

Figure 1. Predicted schematic structure of a two-domain protein consisting of the GT2 domain residing on the cytoplasmic side of the bacterial cell inner membrane and the GH17 domain on the periplasmic side. The eight transmembrane helices are predicted to form a membrane pore through which the newly synthesized glucan chain is transported. According to the hypothetical model, the cytoplasmic GT2 domain produces the linear β-glucan, whereas the periplasmic GH17 domain modifies the nascent β-glucan, following transport through the inner membrane.

e

sized glucan chain, product of GT2, is transported. The periplasmic GH17 enzyme domain may then cleave and further modify the nascent β-glucan synthesised by the GT2 domain, leading to the formation of branched and cyclic OPGs. The schematic structure of the enzyme interacting with the membrane and the synthesis mechanism is illustrated in figure 1. A gene with a similar structure and proposed function has been reported for a two domain protein involved in the synthesis of 1,3-α-glucan in *Schizosaccharomyces pombe (Hochstenbach et al., 1998).*

1.2 Identification of putative one domain bacterial GH17 glycosyltransferases in bacteria

The *Bradyrhizobium japonicum ndvB* gene is located in an operon of three genes (described in more detail in 1.4.3). A second gene in the operon, *ndvC*, also has a domain with homology to GH17 sequences but in contrast to the *ndvB* gene it lacks the GT2 domain. Mutational analysis showed that while this gene was not necessary for the synthesis of cyclic glucans inactivation resulted in reduction or disappearance of 1,6 linkages (Bhagwat et al., 1999). Bhagwat et al (1996) proposed that it added 1,6 linked glucose moieties onto the cyclic backbone. Hydropath profile of the protein revealed a putative signal peptide at the N-terminal and a hydrophobic region at the C-terminal end consisting of apparent seven transmembrane helices. Interestingly, homologues to this gene were also found in almost all the strains containing the two-domain gene (GH17+GT2). The presence of two types of GH17 enzymes in these bacteria indicates functional differences regarding the putative glycosyl transfer of

these enzymes.

1.3 Fungal GH17 glycosyl transferases

Transglycosidase activity at enzyme level of GH17 family members has so far only been reported in the fungal kingdom . A recent study (Gastebois et al., 2010) describes a new fungal β(1–6)/β(1–3)-glucan branching transglycosidase activity in a cell wall autolysate of *Aspergillus fumigatus*. The encoding gene, Af*BGT2* is an ortholog of Af*BGT1*, another transglycosidase of *A. fumigatus* previously analyzed (Mouyna et al., 1998). Both enzymes release laminaribiose from the reducing end of a β(1–3)-linked oligosaccharide and transfer the remaining chain to another molecule of the original substrate. The AfBgt1p transfer occurs at C-6 of the non-reducing end group of the acceptor, creating a kinked β(1–3;1–6) linear molecule.(Gastebois et al., 2010)

The AfBgt2p transfer takes place at the C-6 of an internal group of the acceptor, resulting in a β(1–3)-linked product with a β(1–6)-linked side branch. Sequence analysis showed that AfBgt1p and AfBgt2p belong to the GH17 family. Based on enzymatic, sequence and crystallography data, this family contains β-glucanase and transglucosidases. The active site of the GH17 family enzyme consists of two glutamate residues acting respectively as proton donor and nucleophile residues to cleave β-linked substrates at equatorial bonds and retaining the β-anomeric configuration.

1.4 Novel GH17 β-glucosyltransferases from proteobacteria for modifying linear (β1→3)-linked gluco-oligosaccharide chains

In a previous study of this work, genes encoding β-glucosyltransferase domains of glycosyl hydrolase family GH17 from three species of proteobacteria were cloned and expressed. These were: *Pseudomonas aeruginosa* PAO1; *Pseudomonas putida* KT2440; and *Azotobacter vinelandii* ATCC BAA-1303. The encoded enzymes of these GH17 domains turned out to have a non-Leloir trans-β-glucosylation activity, as they do not use activated nucleotide sugar as donors, but transfer a glycosyl group from a β-glucan donor to a β-glucan acceptor. More particularly, the activity of the three recombinant enzymes on linear β(1-3)linked gluco-oligosaccharides (Lam-Glc_{4-9}) and their corresponding alditols (Lam-Glc_{4-9}-ol) was studied. Detailed structural analysis, based on TLC, MALDI-TOF-MS, ESI-MS, and 1D/2D ^{1}H and ^{13}C NMR data, revealed diverse product spectra, indicating, dependence on the enzyme used, besides β(1-3)elongation activity, also β(1-4) or β(1-6)elongation, or β(1-6)branching activities. All of the enzyme cleaved the substrate from the non-reducing end of the substrate and transferred the new donor end to an acceptor molecule. This was the first characterization of enzymes having such activity from bacteria. A report describing this work is currently in press (Hreggvidsson *et al.* 2010, in press).

1.5 Reaction mechanism

Hydrolysis of glycosides by retaining glycosidases occur via the two-step mechanism involving two carboxyl groups, one functioning as a nucleophile, the other as an acid-base catalyst. In the first step of the reaction, the nucleophile attacks the anomeric centre of the substrate while the acid/base catalyst protonates the departing glycone fragment, leading to the formation of a covalent glycosyl-enzyme intermediate of

inverted stereochemistry at the anomeric centre relative to the substrate. In the second step of the reaction, the acid/base catalyst promotes the attack of the glycone moiety by an acceptor glycone molecule. This attack takes place on the opposite face of the anomeric centre, displacing the nucleophile and releasing the glycone with the same anomeric configuration as the substrate.

Transferases also have two fold reaction mechanisms, but they start by cleaving the saccharide, release a part and retain the other part. The energy from the cleavage is then used to form a new linkage on a new saccharide. It depends on the type of the transferase if the enzyme elongates the saccharide by forming the same type of linkage or forms a new linkage type. The former type of activity is called elongation and the second type branching. The saccharide that is cleaved is designated a donor and the saccharide, which accepts the sugar is designated an acceptor. The rate limiting step is after the enzyme has cleaved the saccharide and it needs another saccharide to be an acceptor (Frey, 1996).

1.6 Cyclic β-glucans

Cyclic β-glucans are unique molecules that are found almost exclusively in bacteria of the *Rhizobiaceae* family. They are a product of glycosyl transferase reaction forming a β-glucan cycle from linear polysaccharides. Reaching concentrations as high as 5 to 20% of the total cellular dry weight under certain culture conditions, the cyclic β-glucans are major cellular constituents. In *Agrobacterium* and *Rhizobium* species, these molecules contain 17 to 40 glucose residues linked solely by β(1-2) glycosidic bonds. However, in *Bradyrhizobium* species, the glucose residues are linked by both β(1-3) and β(1,6) glycosidic bonds. It was proposed that the glucans contained a cyclic β(1-3) backbone of 11 to 13 glucose residues with variable numbers of β(1-6) glucose branch points. These branch points were proposed to serve as primers for the formation of β(1-3)-linked linear branches (Breedveld et. al 1994). The mixture of linkages in *Bradyrhizobium* suggests that the pathway for cyclic β(1-3),(1-6)-glucan synthesis may be different from and more complex than that for the synthesis of cyclic β(1-2)-glucan molecules in *Rhizobium* species (Bhagwat et al., 1996).

1.6.1 Biological function of cyclic β-glucans

A considerable amount of energy is devoted to the synthesis of the cyclic β-glucans, levels of which can reach 20% of the total cellular dry weight in several rhizobia. It does not appear, however, that these glucans function as carbon, phosphorus, or energy reserves for the cell. Studies have indicated that the accumulation of membrane-derived oligosaccharides (MDO, also named osmoregulated periplasmic glucans OPGs), within the periplasm may be advantageous during growth at low osmolarity for the following reasons: (i) the accumulation of these molecules provides a mechanism for the cell to regulate the relative volumes of periplasmic and cytoplasmic compartments; (ii) anionic MDO contribute to the ionic strength of the periplasm, which appears to be important for porin regulation and possibly other processes; (iii) high concentrations of MDO within the periplasm should lead to a reduction in turgor pressure across the cytoplasmic membrane; and (iv) the accumulation of anionic MDO within the periplasm should lead to the development of a Donnan potential across the outer membrane (Breedveld et. al 1994).

The structurally different molecules in *Bradyrhizobium* appear to be functionally equivalent to the cyclic β(1-2)-glucans for hypoosmotic adaptation

(Bhagwat et al., 1996). It may be the cyclic character, not the arrangement of glycosidic linkages, which represents the critical structural feature of these molecules. (Breedveld et al., 1994)

It has been suggested that one way by which pathogens and symbionts can avoid plant defences is by secreting suppressor compounds that prevent these defence responses (Bhagwat et al., 1996). If this is a biological function cyclic β-glucans, how do they suppress a host defence response? Perhaps a mechanism for suppression can be envisioned for the cyclic β(1-6)-β(1-3)-glucans of *Bradyrhizobium* species. The cyclic β-glucans of *Bradyrhizobium* species share structural features with glucan fragments derived from the mycelial walls of fungal pathogens of the soybean plant. These fungal wall glucan fragments have been shown to be potent elicitors of a major defence response of the soybean plant, namely the production of isoflavonoid phytoalexins (Breedveld et. al 1994).

1.6.2 Osmoregulated synthesis of cyclic β-glucans.

Several studies have shown that the biosynthesis of cyclic β-glucans is osmotically regulated in a wide variety of *Rhizobium, Agrobacterium*, and *Bradyrhizobium* strains, with the highest levels of synthesis during growth in low-osmolarity media. This suggests a general role for periplasmic cyclic β-glucans in the hypoosmotic adaptation of the *Rhizobiaceae*. However, this conclusion is complicated by observations that the level of cell-associated cyclic 3-glucans in several strains of *R. leguminosarum* is independent of growth medium osmolarity (Breedveld et al., 1994).

1.6.3 β-glucan biosynthesis genes

Two genes from *B. japonicum*, *ndvB* and *ndvC* that are required for cyclic β (1-3)-β (1-6)-glucan synthesis have been identified. Mutation in either *ndvB* or *ndvC* results in a symbiotically defective microsymbiont (Bhagwat et al., 1999). A mutation in the *ndvB* locus results in a hypoosmotically sensitive strain that is unable to synthesize β-glucans and is symbiotically ineffective. Mutation of *ndvC* results in the synthesis of structurally altered β-glucans, composed almost entirely of β(1-3)-glucosyl linkages. Strains with a mutation in *ndvC* are only slightly sensitive to hypoosmotic growth conditions but are severely impaired in nodule development (Bhagwat et al., 1999).

The nodule development (*ndvB*) gene of *Rhizobium meliloti* and the corresponding chromosomal virulence (*chvB*) gene of *Agrobacterium tumefaciens* encode a large membrane protein that catalyzes the synthesis of the β(1-2)-D-glucan molecules .

The *ndvA* and *chvA* in *Rhizobium meliloti* and *Agrobacterium tumefaciens*, respectively appear to encode an ABC type transporter that allows the transport of the cyclic β-glucans to the periplasmic space (Chen et. al 2002).

Some regions in the putative *ndvC* are strongly similar to regions in β(1-3)-glucanases from tobacco and *Saccharomyces cerevisiae* and a glucanosyltransferase from *Candida albicans*. The deduced amino acid sequence of *ndvC* showed 27% identity (and up to 51% similarity, allowing conservative substitutions) with enzymes involved in β-glucan metabolism from yeast species (Bhagwat et al., 1996). These similarities provide support for the idea that NdvC has a role in synthesis of β(1-3)(1-6)-glucans, perhaps in controlling the addition of β(1-6)-linked units (Bhagwat et al., 1996). The molecular weight of NdvC is 62-kDa and it has several transmembrane domains. Chen et al. 2002 reported a new gene *ndvD* which is located in the region flanked by *ndvC* and *ndvB* in *B. japonicum*, in what appears to be a locus of three monocistronic genes involved in cyclic β-glucan synthesis. A possible role for *ndvD* could be to serve as a

template or effector for *ndvB–ndvC* during β-glucan synthesis. There is no homology between *ndvD* and the other genes (*ndvB–ndvC*) involved in β(1-3),(1-6)-D-glucan synthesis. Thus, *ndvD* apparently is not involved in a general pathway of cellular polysaccharide synthesis (Chen et al., 2002).

1.6.4 Exploitation of cyclic β-glucans

Although the cyclic β-glucans potentially have industrial applications similar to those of the cyclodextrins, it is possible that the rhizobial glucans could find unique applications. For example, the inner cavity diameters of the larger cyclic β(1-2)-glucans (e.g., greater than 18 glucose residues) are predicted to be greater than those of the cyclodextrins. Therefore, the larger cavity diameter of these cyclic β(1-2)-glucans may permit the formation of inclusion complexes with larger hydrophobic guest molecules. Additionally, it is noted that the cyclic β(1-2)-glucans have a greater solubility in water than the cyclodextrins [approximately 250 and 18 g/l for cyclic β(1-2)-glucans and γ-cyclodextrin, respectively] . This property may prove to be of value for certain pharmaceutical or food-processing applications, in which high concentrations of inclusion complexes may be required. (Breedveld et al., 1994)

1.7 Polysaccharides with glucan linkages

1.7.1 Laminarin

Laminarin is a polysaccharide which consists of glucose units that are linked together with a β(1-3) backbone which has β(1-6) linked to the backbone. The ratio between the β(1-3) and β(1-6) is approximately 1:3 (Maeda et al., 1968). Laminarin is usually found in brown algae.

1.7.2 Curdlan

Curdlan is a polysaccharide which consists of glucose units that are linked together with β(1-3) linkage (Nakata, Kawaguchi, Kodama, & Konno, 1998). Curdlan has the degree of polymerisation, (DP) 450 and is the construction without branches. Average molecular weight of Curdlan in 0,3N NaOH is from the range $5.3x10^4$ to $2.0x10^6$ daltons. Curdlan was discovered in 1966 by the professor Harda which named the molecule for its property to curdle when it was heated (Steinbüchel et al., 2005) Curdlan production is mainly from the bacteria *Agrobacterium sp (Stasinopoulos, et. al., 1999) and Alcaligenes faecalis (Jin et. al 2006)*

A good recovery of Curdlan is obtained when the bacteria are cultivated in high glucose feed and is subjected to nitrogen shortage (Stasinopoulos et al., 1999). In nature curdlan is found as a building of a singular helical chains.(Stasinopoulos et al., 1999).

Curdlan has found uses in food industry as a formulation aid, processing aid, stabilizer and thickener or texturizer and was approved by the US Food and Drug Administration (FDA) in December 1996 (Spicer et al., 1999).

Curdlan molecule can reach 12.000 glucose units and is undesolvable in water by can be dissolved in weak base 0,25M NaOH, dimethylsulfoxide (DMSO), formic acid (McIntosh et al., 2005)

1.8 Benefits of β-glucans on health

The effect of curdlan on cancer in people has been investigated, e.g. as biological response modifiers (BRMs) (Kim et al., 2000)

The complex polysaccharides named β-glucans are active compounds with immune activity. β-glucan polymers belong to a class of drugs with effects on the immune

system, such as: anti-tumoral, anti-infectious, protection against fungi, bacteria and viruses infections. (Bădulescu et al., 2009)
Bădulescu et al., 2009 found in his studies that all the investigated curdlan derivatives (SP, Palm CM/SP, CM/SP, Palm CM, Palm SP and CM) were able to inhibit HEp-2 tumour cell growth, by up-regulating Doxorubicin and Actinomycin D cytostatic activity.

1.9 Bacterial sources for GH17 genes used in this study

1.9.1 *Rhodopseudomonas palustris*

Rhodopseudomonas palustris is a purple non-sulphur phototrophic bacterium commonly found in soils and water that makes its living by converting sunlight to cellular energy and by absorbing atmospheric carbon dioxide and converting it to biomass. This microbe can also degrade and recycle a variety of aromatic compounds that comprise lignin, the main constituent of wood and the second most abundant polymer on earth. Because of its intimate involvement in carbon management and recycling, *R. palustris* was selected by the DOE Carbon Management Program to have its genome sequenced by the JGI.

R. palustris is acknowledged by microbiologists to be one of the most metabolically versatile bacteria ever described. Not only can it convert carbon dioxide gas into cell material but nitrogen gas into ammonia, and it can produce hydrogen gas. It grows both in the absence and presence of oxygen. In the absence of oxygen, it prefers to generate all its energy from light by photosynthesis. It grows and increases its biomass by absorbing carbon dioxide, but it also can increase biomass by degrading organic compounds including such toxic compounds as 3-chlorobenzoateto cellular building blocks. When oxygen is present, *R. palustris* generates energy by degrading a variety of carbon containing compounds (including sugars, lignin monomers, and methanol) and by carrying out respiration.

1.9.2 *Methylobacillus flagellatus* KT

Methylobacillus flagellus KT is a part of a group of methylotrophic anaerobic bacteria, and they can be found in large numbers in marine and fresh water ecosystems. These organisms are one of Earth's most important carbon recycler, and they recycle such important carbon compounds as methane, methanol, and methylated amines on Earth. In general methylotrophs can use green-house gases such as carbon dioxide and methane as substrates to fulfil their energy and carbon needs(Bratina et al., 1992)(Chistoserdova et al., 2007)

1.9.3 *Bradyrhizobium japonicum*

Bradyrhizobium japonicum is rod-shaped, gram negative bacteria, which lives a symbiont life with the root system of the soya plant, Glycine max, which harvests nitrogen from the atmosphere. The bacteria forms colonies of cells in the nodular ends in the roots were it receives a safe environment and carbon from the plant. In return the bacteria help the plant to grow by supplying it with nitrogen (Liu et al., 2007).

1.10 Alignment of GH17 amino acid sequences

In the beginning of this study, amino acid sequences of GH17 protein domains were extracted from databases and aligned. The enzymes were classified according to their domain structure. Type I glycosyltransferases are comprised of two different domains N terminal GH17 and C terminal GT2 domain connected with hydrophobic amino acids. Type II transferases only have the GH17 domain with hydrophobic amino

acids at the C-terminal end. A phylogenetic tree was made from amino acid alignment of selected GH17 sequences of both types (Figure 2). According to the results, Type I and Type II GH17 domain-sequences cluster on separate branches. This clear divergence of Type I and Type II enzymes and the fact that the two types co-exist in the bacteria supported the notion that two separate types of GH17 domains may have evolved towards different glucosyl-transferase specificity.

One of the two domain genes revealed in the BlastX search, *ndvB* from *Bradyrhizobium japonicum* had previously been shown to be essential for the synthesis of cyclic glucans by complementation and mutational analysis. As previously mentioned, this *ndvB* gene was a part of an operon of three genes in this species. A second gene in the operon, *ndvC*, also had a domain with homology to GH17 sequences but in contrast to the *ndvB* gene it lacked the GT2 domain. Studies have shown that the *ndvB* participate in the formation of the β(1-6) linkages (Chen et al., 2002).

Therefore it was decided to examine further the GH17 domain of both types, of three different species. *Bradyrhizobium japonicum* was chosen as it had shown it possesses the ability to form a new the β(1-6) linkages. Also, two other species of type II were chosen, one that was closely related to the *B. japonicum*, i.e. *Rhodopseudomonas palustris* (see figure 2), and another more distantly related, *Methylobacillus flagellatus KT*

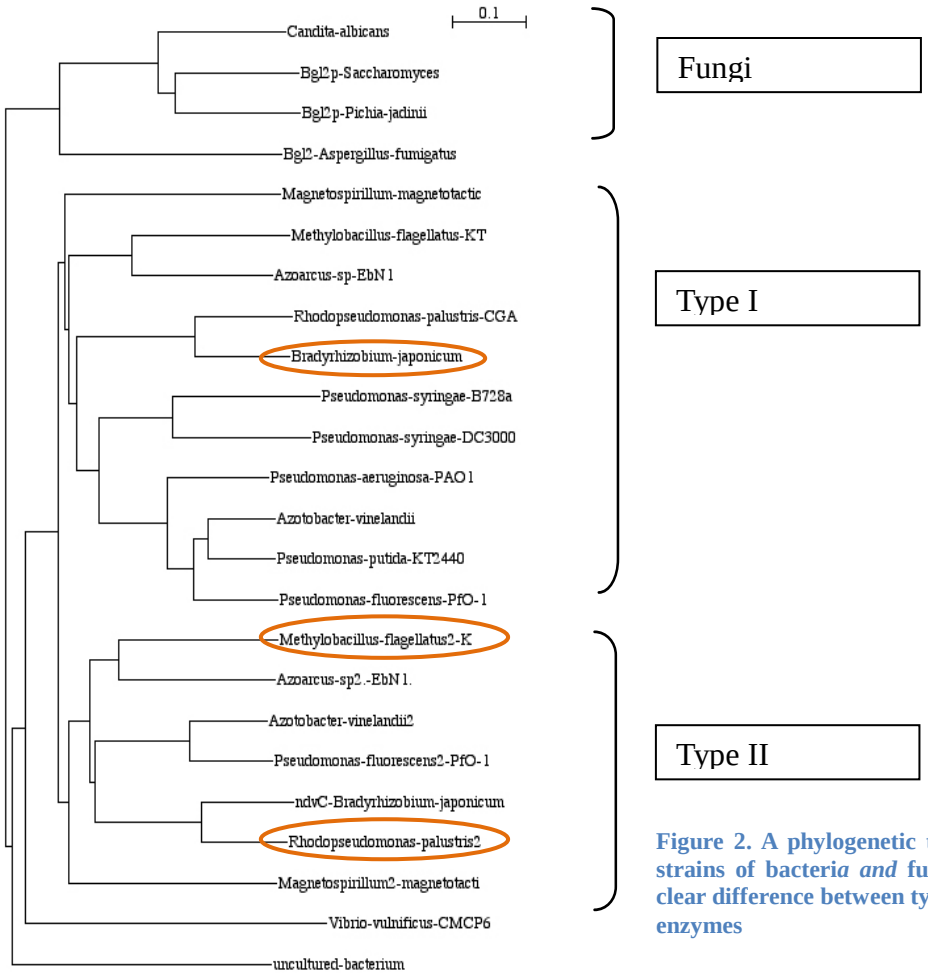

Figure 2. A phylogenetic tree of different strains of bacteri*a and* fungi. There is a clear difference between type I and Type II enzymes

1.11 Analytical methods to study β-glycan enzyme products

To be able to get information about the size and the linkage type of the products, three different methods were used NMR (nuclear magnetic resonance), MALDI TOF (Matrix Assisted Laser Desorption Ionisation with Time of Flight detection) and Electrospray MS. These studies were done at the University of Utrecht in Holland.

The problem facing the examination of the products is that the substrate is a big portion of the mixture and it may interfere with the analysis. It is therefore necessary to purify the reaction to substrate and products by utilizing gel filtration.

1.11.1 TLC

It is possible to use TLC to distinguish between different size and charge of oligo saccharides. To be able to interpret the different spots formed on the plate a standard is necessary. The most common material used for TLC plates is silica gel (Zubrick, 1997).

1.11.2 NMR

The best quality of the NMR technology is that the method is not intrusive because it does not destroy the sample, and is possible to detect accurately the structure of the oligo saccharides. The down side is that a rather high quantity of sample is needed to be able to establish a clear picture of the branching type by doing a 2-d analysis with for instance TOSKY and ROESY, Rotational Frame Nuclear Overhauser Effect Spectroscopy. ROESY is a part of the Overhauser Effect is the transfer of spin polarization from one spin population to another via cross-relaxation in nuclear magnetic resonance (NMR) spectroscopy Ordinary analysis with 1H NMR does not enquire a lot of material. Also, a lot of experience is needed to interpret the results as NMR spectra can be complicated. Structure of the oligosaccharide can be established by doing a comparison of the NMR spectra with known samples (Merry, 1999)

To be able to interpret the NMR spectra, a study by Y. Kim et al., 2000 was used to help by the examination of the β-D(1-3)(1,6)-linked glucans. Protons H-2, H-3, H-4, H-5 and H-6 of the backbone resonate in the same frequency. It was easy to separate these protons with the help of COSY, Correlation spectroscopy**,** and HMQC, Heteronuclear Multiple Quantum Coherence, graphs. Two-dimensional NMR spectra provide more information about a molecule than one-dimensional NMR spectra and are especially useful in determining the structure of a molecule, particularly for molecules that are too complicated to work with using one-dimensional N. During some of the delays in COSY experiments, the nuclear spins are allowed to freely precess (rotate) for a determined length of time known as the evolution time. The frequencies of the nuclei are detected after the final pulse. By incrementing the evolution time in successive experiments, a two-dimensional data set is generated from a series of one-dimensional experiments. HMQC are 2D inverse correlation techniques that allow for the determination of connectivity between two different nuclear species http://en.wikipedia.org/wiki/Correlation_spectroscopy

1.11.3 Electrospray MS

Electrospray MS usually gives a good graph but it can be hard to interpret microheterogeneity (Merry, 1999)

To interpret the peaks from the electrospray a convenient way is to use a system that (Domon et al., 1988) set to indicate were the saccharides break up. In this system the ions form is given a letter based on were the breakage occurs. If the saccharide breaks from the non-reducing end then it will receive the letters B or C, depending on which side of the oxygen the breakage is. Also used for this system is numbers which indicate what glucose unit the breakage is. If the saccharide is from the reducing end it will get the letters Z or Y with a number which indicates how close to the reducing end the breakage is. But if there is a breakage inside a glucose ring then it gets the letters A or X depending on from which end the cleavage is. $^{3,5}A_1$ tells that the first glucose from reducing end broke and it was linkage 3 and 5 that broke, see Figure 3. With the development and ease of the Electrospray and Maldi TOF advances it will make it possible to determine the molecular weight with the information of the sugar composition, linkage type by examining the brake down products. (Reis et al., 2004)

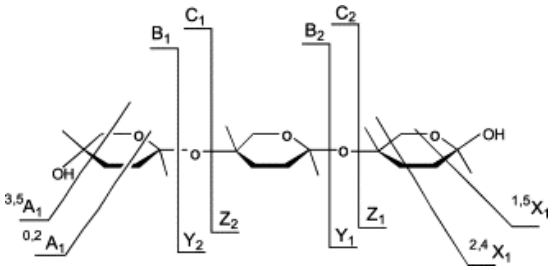

Figure 3. The figure shows how a saccharide can possibly brake up and how the peaks are assigned with respect to the breakage linkage (Domon et al 1988)

These analytical methods can be performed by examining the saccharide straight or by treating it before by permethylating the saccharide. The reason for permethylering the saccharides before they are applied to mass specs is that there methyl groups are added instead of hydroxide and the pattern how the saccharide breaks gives insight into the linkage of the saccharide.

1.11.4 Maldi TOF

Maldi TOF has changed how polysaccharides are examined by making it possible to ionize polysaccharide or glycoproteins. The main concern is to make sure that the products are pure from any contamination for example salts that can interfere with the ionization. Also a lot of experience is needed for interpreting the results. Brake through has been in diagnostics of saccharides with MALDI TOF as the prize of these equipment has lowered with the development of better matrixes which are better suited for these studies, e.g. α-cyano-4-hydroxycinnaminic acid and 2,5-dihyhydroxybenzoic acid (Merry, 1999)

After the sample has been purified with for instance Micro-columns with ion exchange or another type of column material then the sample is mixed together with the matrix and re-crystallized for analysis. Ionisation is achieved with the sample absorbing energy from the laser and monitored through the time of flight. The mass is measured and compared with a calculated values of different mono saccharides (Merry, 1999)

By applying the methods described above and by investigating the bread up products it is possible the deduce the type and the location of branches on the polysaccharides

It is possible to determine were the branch point occur in polysaccharides by examining how they break apart in Maldi (Reis et al., 2004)

2. Material and methods

2.1 Bacteria strains

Bacterial strains used in this study as a source of glycosyl transferase genes were the following. *Methylobacillus flagellatus* KT (DSMZ6871), the source of glt13, *Rhodopseudomonas palustris*(DSMZ126), the source of glt9, *Bradyrhizobium japonicum*(DSMZ1755), *the* source of glt20. All strains were obtained from DSMZ, the German collection of Microorganisms. *Escherichia coli*, BL(21) plys, was used for the cloning experiments (Dai et al., 2002).

2.2 Bacteria medium and antibiotics

2.2.1 L-medium

10g Trypton, 5g yeast extract with 10g NaCl í 1L dH_2O. Media allocated into 50mL Erlenmeyer flask and autoclaved at 121°C (Sambrook et al., 1989)

2.2.2 SOC medium

2% Trypton; 0.5% yeast extract; 10mM NaCl; 2.5mM KCl; 10mM $MgCl_2$; 10mM $MgSO_4$; 20mM Glucose. (Sambrook et al., 1989)

2.2.3 Agar plates

15g of agar was added to 1L of L-medium. Before the agar hardens ampicillin was added to the plates for the final concentration of 100µg/mL.

2.2.4 Antibiotics

Stock solution of ampicillin was prepared by dissolving 100mg in 1mL of dH_2O and sterilized through 0.45µm Millipore filter. The concentration of the stock was 100mg/mL.

2.3 The cloning of genes from strains

The domain encoding gene sequences were amplified by PCR using a proof reading polymerase (Platinum Pfx from Invitrogen), purified chromosomal DNA as a template, and the primers listed below. The forward primers were targeted 30-40 bp downstream of the start codon of the orf, thus excluding sequences encoding hydrophobic amino acids of N-terminal signal peptide sequences. The reverse primers were targeted at sequences encoding amino acids at the C-terminal boundary of the GH17 domain and a downstream transmembrane helices region, predicted according to sequence alignment.

The primer pairs for the amplification of *glt9* from *Rhodopseudomonas palustris* were:

Glt9-d64-f2 5'GCCAGCAAGGGCGAGGCCATGATCTTCGGTGTG3'
Glt9-hind-r 5'CCCCAAGCTTAGCCCGCCGGATACTTCTC3'

The primer pairs for the amplification of *glt13* from *Methylobacillus flagellatus* KT were:

Glt13-d18-link-f 5'GCCAGCAAGGGCGAGGCCGACTGGTTCTGGC AGCAAAAC3'
Glt13-hind-r2 5'CCCAAGCTTACCCCGTGAATTCAAACTTGC3'

The primer pairs for the amplification of *glt20* from *Bradyrhizobium japonicum* were

Glt20syn-link	5’GCCAGCAAGGCGAGATGGCAGGTTATGGGGG3’
Glt20-synt-hin	5’GCCCAAGCTTATTCAACCGGACCTGTCCA3’

2.4 Cloning and expression system

An *E .coli* expression vector from Motejadded et al. 2009 was used for the cloning and expression of the glycosyl transferase and to facilitate the purification of the recombinant enzymes. The gene expression is inducible with L-Rhamnose. The insert can be fused with a maltose binding domain sequence and His-tag for affinity purification, *Saccharomyces cerevisiae* Smt3 domain sequence, optimized for the expression in *E. coli*, is located between the maltose binding domain sequence and the cloned gene. .

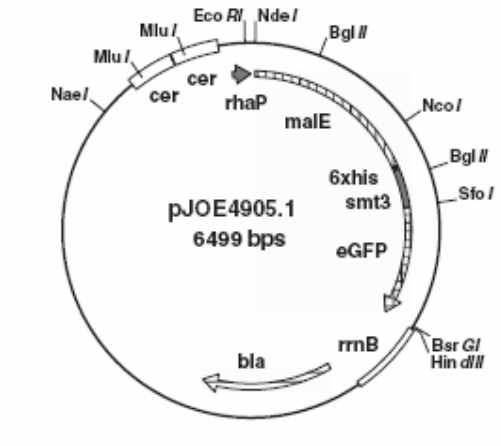

Figure 4. A restriction map of the cloning vector used.

For the use of the system it was important to cultivate and purify Ulp1 protease which cleaves the fusion protein at the Smt3 site.

Ulp1-Sumo protease is constructed from 621 amino acids (AA) which contains two domains. The domain on the C-terminal is a well conserved protease domain (432-621). The second domain on N-terminal is not a well conserved. (Mossessova et al., 2000)

The active part of the protease Ulp1 is similar the other cystein protease. Nucleophilic cysteine (Cys-580) is controlled by the base (His-512), which is stabilized by Asp-574. There is a shallow and tight tunnel VDW(valine, aspartic acid and tryptophan) which recognise the Smt3 Gly-Gly linkage (Mossessova et al., 2000). The benefits of using the Ulp1 protease is that is recognise the 3-dimensional construction of the Smt3 but not the sequence. By utilizing this character of the protease, it is possible to control that the protease only cuts between the domains and not in the cloned enzyme (Motejadded et al., 2009).

2.5 PCR

For the amplification of the *glt* genes from the three different bacteria, the following solution was prepared

PCR for glt 20

0.8µL	100pmol/µL Forward primer
0.8µL	100pmol/µL Reverse primer
1µL	$MgSO_4$
4µL	10mM dNTP
5µL	10x Reaction buffer
0.5µL	2.5U/µL PFX polymerase
2µL	Enhancer solution
1µL	DNA template
38.5µL	dH_2O

The PCR profile was as following for glt 20

94°C for pre denaturation of the template DNA
The cycle of three steps repeated 30 times
94°C for 50 sec denaturation
50°C for 50 sec annealing
68°C for 60 sec elongation
A final incubation at 68°C was done to complete elongation
Subsequently the mixture was cooled down to 14°C until the DNA was loaded on gel

PCR for *glt9*

0.8µL	100pmol/µL Forward primer
0.8µL	100pmol/µL Reverse primer
1µL	10mM dNTP
5µL	10x Reaction buffer
0,5µL	2.5U/µL PFX polymerase
2µL	DNA template
39.9µL	dH_2O

The PCR profile was as following for *glt 9*
94°C for pre denaturation of the template DNA
The cycle of three steps repeated 30 times
94°C for 50 sec denaturation
50°C for 50 sec annealing
72°C for 60 sec elongation
A final incubation at 72°C was done to complete elongation
Subsequently the mixture was cooled down to 14°C until the DNA was loaded on gel

PCR for *glt 13*

1µL	100pmol/µL Forward primer
1µL	100pmol/µL Reverse primer
1µL	$MgSO_4$
4µL	10mM dNTP
5µL	10x Reaction buffer
0.5µL	2.5U/µL PFX polymerase
2µL	Enhancer solution
1µL	DNA template
34.5µL	dH_2O

The PCR profile was as following for *glt 13*
94°C for pre denaturation of the template DNA
The cycle of three steps repeated 30 times
94°C for 50 sec denaturation
56°C for 50 sec annealing
68°C for 60 sec elongation

A final incubation at 68°C was done to complete elongation
Subsequently the mixture was cooled down to 14°C until the DNA was loaded on gel

2.6 Electroporation of DNA in agarose gel.

Routinely a 25mL of 1%(w/v) agarose gel with 1µL of ethium bromide to examine DNA bands. The running condition used were 80 Volts for 40 minutes and the DNA was visualized by using UV light in a Gel Doc 2000 from Bio-Rad.

The standard used was 1kB ladder from New England Biolabs part no. NEB #N3232 a picture of the standard is in the appendix.

The loading buffer was as followed:

4mL	0.5M EDTA pH 8,0
22.52mL	87%Glycerol
13.28mL	dH_2O
0.02	Bromophenyl blue

10µL of sample was added to 7µL of loading buffer and everything was loaded to agarose gel.

Isolation of PCR product from agarose gel

To isolate pure DNA from agarose gel a kit from GE Healthcare Illustra™ GFX™ PCR DNA and Gel Band Purification Kit part no. 28-9034-71 was used. Isolation was done according to instruction. The following volumes were used:

280µL Capture buffer
500µL Wash buffer
20µL dH_2O

2.7 Digestion of DNA with restriction enzymes

Bacterial DNA PCR amplification and vector, pJOE4905, were digested with restriction enzymes at 37°C over night. The reaction volumes and composition were as followed:

For all three different clones the same volumes and restriction enzymes were used

PCR amplification

10µL	125ng/µL GFX product
3µL	NEB2 buffer
1µL	20.000U/mL restriction enzyme, Hind III
16µL	dH_2O

Vector

20µL	pJOE 4905 (500 ng)
4µL	NEB2 buffer
1µL	20.000U/mL restriction enzyme Hind III
1µL	10.000U/mL restriction enzyme, SFO I
14µL	dH_2O

2.8 DNA ligation

Ligation of sample and control were carried out at 16°C over night.

1.00µL	Vector pJOE 4905 after restriction ~100 ng
6.00µL	Sample DNA after restriction
0.25µL	400.000U/mL DNA T4 ligase
1.00µL	10x reaction buffer
1.75µL	dH_2O

2.9 Transfer of plasmids into *E. coli* cells

Escherichia coli BL21 strain Pri3715, were used as host cells for the transformation For transformation 1µL of the ligation was taken and mixed together with the cells. The cells were electro-pulsed with a Gene-pulser from Bio-Rad, 25µF; 1,25kV og 200Ω, after the electro-pulse the cells were placed in SOC medium and grown at 37°C for 1 hour at 10.000 rpm shaking. After incubation in SOC medium for one hour 50, 200µL of cells were spread onto agar plates containing L-medium with ampicillin. Plates were grown over night at 37°C

2.10 Enzyme production and purification

2.10.1 Cultivation of Cells and induction of enzymes

Cells were cultivated in 30mL L-medium containing 30µL 100mg/mL ampicillin, at 37°C with 200rpm shaking. When the absorption of the cells reached OD600nm 0.8 - 0.9 after approximately 4 hours, the cells were induced by adding 300µL of 10mg/mL L-Rhamnose. Then the cells were cultivated over night at 22°C and 200rpm.

2.10.2 Disruption of cells

After cultivation the cells were spun down at 4.300g in a Beckman Coultter TJ-25-centrifuge with TS-5.1-500 bucket rotor. Supernatant was discarded and the pellet weight. The pellet was dissolved in amylose binding buffer so the final concentration was 0,2g/mL. Cells were disrupted in a sonicator from Branson, sonifier 250, 1 minute, duty cycle 40%. Cells were kept on ice throughout the process.

2.10.3 Production of crude extract

After the disruption of the cells, the cell debris was spun down at 13.200rpm for 5 minutes at 4°C. The supernatant was collected and filtrated through 0.45µm filter from Millipore, before the sample was loaded onto a column.

2.10.4 Protein purification on a Amylase column

Amylase column was packed according to the instruction from the manufacturer. The column matrix was amylose resin from New England Biolabs with the purchase number EB021S. The material was packed into Tricon™ 10/50 column from Amersham bioscience, purchase number 18-1163-14. The column was run on FPLC Akta purifier from Amersham. Flow rate was 0,8mL/min and the gradient was from 0 to 100% of elution buffer for 5 column volume, CV. The concentration of the elution buffer is increased linearly over 5 column volumes. The Binding buffer consisted of 20mM Tris pH 7.6; 200mM NaCl. The elution buffer consisted of 20mM Tris pH 7.6; 200mM NaCl; 10mM Maltose

2.10.5 ULP protease cleavage

In order to cleave the maltose binding domain from the enzyme a ULP protease (Motejadded et al., 2009) was used. The ULP protease clone was cultivated and the

protease was purified on His trap column from Amersham in house. The sample from the amylose column was pulled together and desalted on 5mL HiTrap™ Desalting column from GE healthcare, purchase number 17-1408-01, into ULP buffer which consisted of: *50mM Tris pH 8@30°C; 150mM NaCl; 1mM di-thiolthreitol: 0.1% Triton x-100*

10µL of 0.1mg/mL ULP protease was placed in 1mL sample. Reaction was run 4hours at 30°C.

2.10.6 HisTrap purification

After ULP protease treatment the sample was desalted on 5mL desalting column into HisTrap binding buffer. Sample pulled together and applied on 5mL HisTrapFF Chelatin column charged with 0,5mL 0,1M $NiSO_4$ from GE healthcare, purchase number 17-5255-01. Flow through from the column was collected and desalted on 5mL desalting column into storage buffer. Following buffers were used.
Binding buffer: 20mM $NaPO_4$ pH7.6; 500mM NaCl; 10mM imidazole
Elution buffer: 20mM $NaPO_4$ pH7.6; 500mM NaCl; 500mM imidazole
Storage buffer: 20mM $NaPO_4$ pH7.0; 150mM NaCl

2.11 SDS-Page electrophoresis

Protein purification and expression were routinely done by examining protein band on 10%(w/v) (Laemmli, 1970). SDS-Page were cast in 10x10.5 cm glass from Hoefer™ miniVE Amersham. Protein standard was from New England Biolabs and the range of the marker was from 2 to 212kDa purchase number P7702S.

Following buffers were used for the electrophoresis:

SDS loading buffer
4mL 1M Tris/HCl pH 6.8
800µL 0,5M EDTA
0.77g SDS
8mL 50%Glycerol
0.005% Bromophenyl blue

Before use 50µL of mercaptoethanol was added to 950µL of SDS loading buffer. Routinely 10µL of sample was boiled with 3µL loading buffer, before the sample was applied to the SDS gel.

5L Tank buffer
15.1g TrisHCl pH 8.0
72g Glycin
5g SDS
dH_2O fill to 5L

4% Stacking gel
5mL dH_2O
3mL Stacking buffer, 0.5M Tris HCl pH 6.8
4mL 40% acryl amide bis from Sigma
116µL 10% SDS,

58µL 10% AMPS
6µL TEMED

10% Resolving gel
2.9mL dH_2O
1.5mL Resoling buffer, 1.5M Tris HCl pH 8.5
1.4mL 40% acryl amide bis from Sigma
60µL 10% SDS,
60µL 10% AMPS
2.4µL TEMED

Routinely, 10µg of protein were applied to the SDS-Page. Gels were run at 200W, 100V and 25mA for 2hours.

2.11.1 Bradford quantification of proteins

Protein concentration was determined with the Bradford reagent from Bio-Rad (Bradford, 1976), purchase number 500-006. The method was standardized with bovine serum albumin, BSA, in concentration from 0.1 to 1mg/mL. To determine the absorbance, a spectrophotometric reader from Tecan Sunrise, which can read 96 plates at 595nm, was used. For the absorbance measurements, following mixture was prepared:

10µL Sample / water used as a blank
160µL dH_2O
40µL Bradford reagent.

Following mixing, a care was taken to prevent formation of air bubbles and the absorbance was read immediately. Protein concentration was determined from a standard curve of BSA.

2.11.2 Visualization of protein bands in SDS-Page

SDS gels were stained according to the Fairbanks protocol described by (Wong et al., 2000). Gels were placed in plastic container which is considered microwave safe. The gel was incubated in Fairbanks solution A so as the solution covered the gel and heated for 1 minute at 800W in the microwave, the gel was allowed to cool down with gentile shaking. After the gel cooled down, the solution A was discarded and solution B was placed over the gel, in the microwave at 800W for 1 minute and the solution immediately discarded. Solution C placed over the gel, in the microwave at 800W for 1 minute and the solution immediately discarded. In the final step, the gel was covered with solution D and heated for 1 minute at 800W the gel allowed to cool down with gentile shaking. Gels were stored by sealing them in plastic bags with a sealer. After sealing, the gels were scanned into a computer with a Canon scanner. The recipe for the Fairbanks solutions is the following:

Fairbanks solution A
0.05%(w/v) Coomassie brilliant blue R250
25%(v/v) Isopropanol
10%(v/v) Acetic acid

Fairbanks solution B
0.005%(w/v) Coomassie brilliant blue R250

10%(v/v) Isopropanol
10%(v/v) Acetic acid

Fairbanks solution C
0.002%(w/v) Coomassie brilliant blue R250
10%(v/v) Isopropanol
10%(v/v) Acetic acid

Fairbanks solution D
10%(v/v) Acetic acid

2.12 Preparation of oligo saccharides

Oligosaccharides used for the enzyme assays were purchased from Megazyme. The product sheet stated that the oligosaccharides were at least 98% purity. The oligosaccharides were prepared from laminarin and the size range from biose to hexose. The oligosaccharide purity was not sufficient so it became necessary to purify them further before use.

Figure 5. The old titration pipette filled with bio-gel P2

For the purification, a bio-gel P2, product number 150-4115, was prepared and packed. The column material was packed according to the manufacture specification. The column was from an old titration pipette with a broken valve. The end was sealed off with a disk from BioRad. The size of the column was 1.5cm x 1.5m. The column was run at 0.2mL/min (see Figure 5).

The column was calibrated with Blue Dextran2000 from Pharmacia Biotech, product number 17-0442-01, to establish the void volume of the column. The Running buffer was 10mM Ammonium bicarbonate.

The fraction were collected based on these information, collection of fraction took place after the time it took the blue dextran to pass through the column. For the tests a 500µL of sample were collected in Eppendorf tubes. The samples were freeze dried and examined on TLC.

Further, pure oligosaccharides were obtained from curdlan and were produced in the University in Utrecht, Holland, courtesy of Justina M. Dobruchowska.

2.13 Reduction of oligosaccharides

In order to reduce the oligo saccharides from aldehyde to alcohol a procedure from a chapter about chemical labelling of carbohydrates by oxidation and sodium borohydrate reduction section 17.5.1 from the book, Current protocols in molecular biology volume 3(Ausubel et al., 2001) was followed. Minor modification was done on the protocol as we used non-radioactive sodium borohydrate.

The oligosaccharides were dissolved to the final concentration of 5 mg/mL, and then $NaBH_4$ was added to the final concentration of 5mg/mL. The reaction was done at room temperature for 2 hours. After the reaction excess $NaBH_4$ was neutralized by adding to the reaction 4M acetic acid until the pH of the solution was 6 according to litmus paper. The solution with methanol added was evaporated with freeze drying,

Heto lyolab 3000.

2.14 Thin Layer Chromatograph (TLC)

Progress and examination of purity of the oligo saccharides were examined with TLC aluminium plates 20x20cm silica gel 60 F_{254} from Merck, product number 1.0554.0001. The plates were loaded with 2µL of reaction products, samples allowed to dry and the plates placed in TLC chamber from Sigma. The running buffer was 1:1:2 dH_2O : acetic acid : butanol.

The plates were incubated in the chamber for 4 hours. The plates were dried and developed with 2%(v/v) aniline[62-53-3] from Sigma, 2%(w/v) di-phenylamine [122-39-4], 16.6%(v/v) 85% phosphoric acid dissolved in acetone (Anderson, et al., 2000). This solution prepared fresh every day. TLC plate was dipped into development solution and placed in 100°C heating cabin for 10 to 15 minutes.

2.15 Enzyme reaction

2.15.1 Aldehyde activity measurement

Activity of the enzyme was routinely assayed under the following condition:
10µL 6.25mg/mL Laminarin Hexose
3µL 0.5M KPO_4 pH 6.5
21µL Enzyme
The mixture was incubated for 3 days at 37°C. Progress of the reaction was monitored by spotting a sample onto TLC plates.

2.15.2 Alditol activity measurement

Activity of the enzyme was routinely assayed under the following condition:
10µL 6.25mg/mL Laminarin Hexose reduced to alditol.
3µL 0.5M KPO_4 pH 6.5
21µL Enzyme
The mixture was incubated for 3 days at 37°C
Progress of the reaction was monitored by spotting a sample onto TLC plates.

2.16 Maldi TOF analyses of oligosaccharides

Matrix-assisted laser desorption ionization time-of-flight mass spectrometry (MALDI-TOF-MS) experiments were performed using a Voyager-DE PRO mass spectrometer (Applied Biosystems) equipped with a Nitrogen laser (337 nm, 3 ns pulse width). Positive-ion mode spectra were recorded using the reflector mode and delayed extraction (100 ns). Accelerating voltage was 20 kV with a grid voltage of 75.2%. Acquisition mass range was 550-3000 Da. Samples were prepared by mixing on the target 1 µL 6.25 mg/mL oligosaccharide substrate solution with 2 µL aqueous 10% 2.5-dihydroxybenzoic acid as matrix solution.

2.18 NMR analyses of oligosaccharides

Resolution-enhanced 1D/2D 500-MHz 1H NMR spectra were recorded in D_2O on a Bruker DRX-500 spectrometer (Bijvoet Center, Department of NMR Spectroscopy, Utrecht University) at a probe temperature of 335K. Prior to analysis, samples were exchanged twice in D_2O (99.9 atom% D, Cambridge Isotope Laboratories, Inc., Andover, MA) with intermediate lyophilization, and then dissolved in 0.6 mL D2O. Chemical shifts (δ) are expressed in ppm by reference to internal acetone (δ 2.225 for 1H). Suppression of the HOD signal was achieved by applying a WEFT pulse sequence for 1D experiment. HOD signal is apparent when D_2O interacts with the charged OH group these interactions influence the neighbouring atoms, so that changes in chemical shift occur. (Michell et al., 2007).

Kim et al., 2000 did a study of different types of saccharides. For the gentabiose (see Figure 6), the α-H-1 and β-H-1 on the reducing end located at á 4.96ppm (d, J 3.7Hz) and 4.34ppm (d, J 7.9Hz). Proton H-1 on the second glucose unit formed a duplex at 4.23 ~ 4.26 ppm because of the two anomeric forms at the reducing end. Coupling constant for the H-2 proton for the COSY graph corresponds with the C-1 carbon in the HMQC graph.

For laminarin pentose and laminarin heptose, a six H-1 resonance peak which forms a doublet at 4.41 ~ 5.04 ppm α- and β-H-1 protons were located at 5.03ppm (d, J3.6Hz) and 4.43 ppm (d, J 7.7Hz). Biggest peak at 4.57 ppm (d, J 7.8Hz) was formed by H-1 protons, which were located at the inner glucose units. Peak forms a triplet at4.50 ~ 4.53 ppm but are in reality two doublets from the second glucose unit closest to the reducing end.

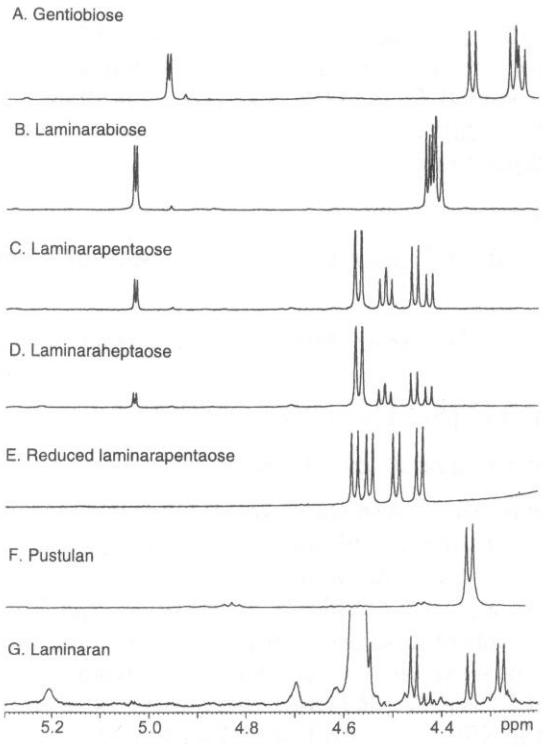

Figure 6. Diffrent NMR graphs of diffrent size and linked oligos and the effect on the NMR spectra (Kim et al., 2000)

2.19 Electrospray analyses of oligosaccharides

The free oligosaccharide-alditols/reaction products were analyzed using an LCQ DecaXP ion-trap mass spectrometer equipped with an electrospray ion source (Thermo Finningan, San Jose, CA). The samples were dissolved in the mobile phase, methanol/water (1:1) to a concentration of approximately 180 ng/µL and then were introduced via a syringe pump at a flow rate of 3 µL/min. The capillary temperature was set to 200 ºC. ESI mass spectra were acquired in the positive-ion mode by scanning over *m/z* 50-3000 with a spray voltage of 3.0 kV and varying capillary voltage of 35 to 50 V. Tandem mass spectra were obtained using automated MS/MS by isolating the base peak (parent ion).

3. Results

The results will be reviewed for each enzyme separately in the following sections.

3.1 Glt 9 from *Methylobacillus flagellates*

3.1.1 Cloning and expression

The amplification of the DNA sequence gave a strong and visible band on a agarose gel and the size of the amplified DNA was correct. The expected size for glt 9 gene was 876bp. Several transformants containing *glt9* in pJOE3075 were obtained. Following expression cultivation, the cell extracts were run on SDS gels to evaluate the expression. From the SDS gel it is clear that the expression was quite good but expected size of the clone was around 31,5kDa + MalE domain (56kDa), i.e. the size of the combined enzyme with Mal E domain was 87,8kDa. The expression is around 15% of the total protein by visual inspection of the gel. The expression of the enzyme was considered successful.

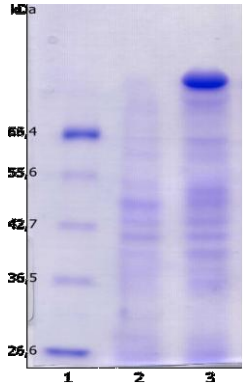

Figure 7. SDS-page gel showing the results of the expression of glt9. 1. Ladder, 2. Negative control, empty cells 3715. 3.glt9 after induction

3.1.2 Purification

Supernatant from cell eruption was collected after sonification and filtrated through 0.45µm filter before a 1mL of supernatant was loaded onto 5mL amylose column. Flow through and peaks from the column were collected into tubes with a fraction collector.

Peak fractions from A3 to A8 were collected together and 1,5mL of that solution was desalted through 5mL desalting column in ULP buffer. Peaks from the desalting column were pooled, 200µL from the desalted column was added to 20µL 0,1mg/mL ULP protease, reaction was done at 30°C and 480rpm overnight. The Ulp1 protease cleaved the MalE domain from the GH17 Glt13 domain. The enzyme domain was then separated from the MalE domain by running the digestion products on a His column, which immobilized the MalE domain. The purified enzyme was used in subsequent enzyme reactions.

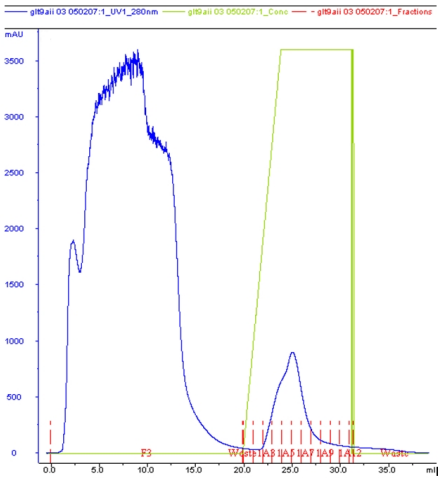

Figure 8. The purification of Glt9 clone on amylose column. Fractions A3 to A8 were pulled together and continued with further studies

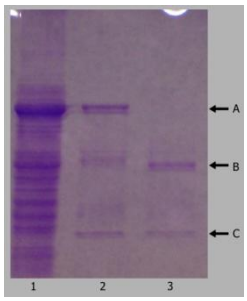

Figure 9. 10% SDS gel of Glt9 crude extract and purification fractions. (1) Sample on amylose column. (2) Sample after amylose column. (3) Sample after ULP reaction. The arrows point to the following bands: (A) Enzyme with MalE domain. (B) MalE domain. (C) GH17 Enzyme Glt 9

3.1.3 Activity analysis TLC

The enzyme was incubated with laminarin substrate as described in material and methods. After the enzyme reaction had progressed for 3 days on laminarin hexose, 2µL from the reaction was spotted on TLC plate and the plate developed. As Figure 10 shows then the main products from the reaction are DP7 and DP5, Also visible were sizes DP4 and DP8. The products from the reaction were purified on Biogel P2 column and the products analysed further with NMR and Maldi TOF

By looking at the TLC, see Figure 10, at lane A it is clear the enzyme is producing a bigger oligo saccharide and the size is at least one glucose unit bigger. Also there is a visible a smaller oligo saccharide which is also one glucose unit shorter. Also faintly visible are a larger oligosaccharide which appears to be the glucose units bigger and a smaller oligo which appears to be two glucose units smaller.

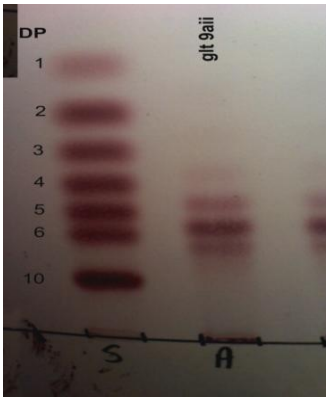

Figure 10. The reaction of Glt9 with laminarin hexose over the course of three days. The Glt9 reaction is in lane marked the the letter A. In the lane S is a standar dand the size is indicated beside the lstandard. Glt 9 is producing a bigger saccharide of at least one dp as seen in the TLC and also producing a smaller oligo

3.1.4 MALDI-TOF-MS

3.1.4.1 Aldehyde oligosaccharides

MALDI-TOF-MS analysis of DP6 products revealed a major [M+Na]+ peak at m/z 1175.3, corresponding with Hex7 and three minor [M+Na]+ peaks at m/z 1013.3, 1337.4 and 1499.4 corresponding with Hex6, Hex8 and Hex9, but it not clear at this stage what linkage type there are involved. But is clear that the main product is Hex7 which is at least 2 times higher intensity than Hex8 and 10 times higher intensity then Hex9 . From these data it is easy to postulate that the substrate is increasing by one glucose unit. As the reaction progresses a higher mass is observed.

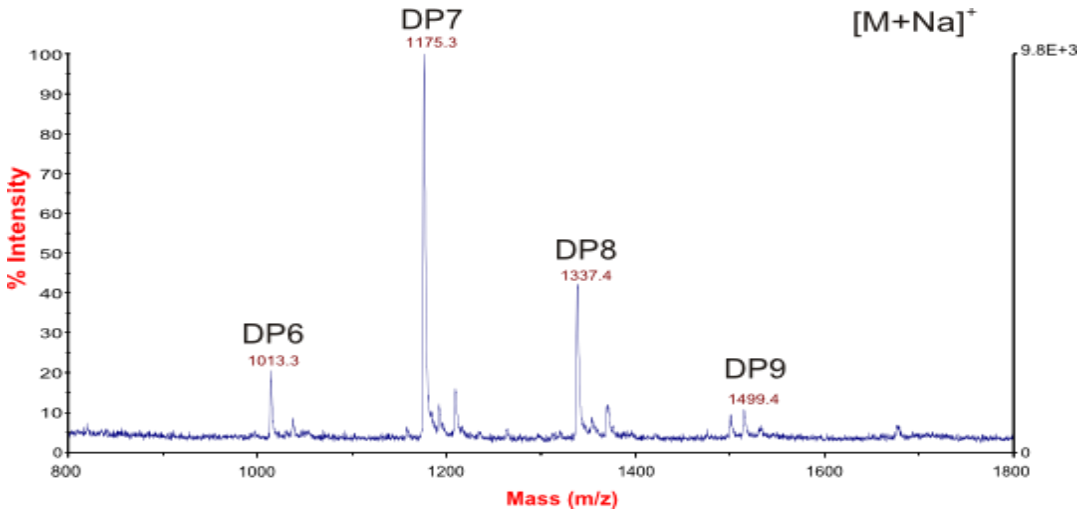

Figure 11. A NMR for the aldehyde product after Bio-gel purification. The substrate was DP6 and there are clearly bigger oligosaccharides visible and the size of them are Hex_7 , Hex_8 and Hex_9 . There is a clear pattern here but the Hex_7 is approximately 2 times bigger than Hex_8 and 10 times bigger than Hex_9

3.1.4.2 Alditol oligosaccharides

MALDI-TOF-MS analysis of DP6-ol products revealed a major [M+Na]+ peak at m/z 1339.4, corresponding with Hex8 and three minor [M+Na]+ peaks at m/z 1177.4, 1501.5 and 1663.5 corresponding with Hex7, Hex9 and Hex10

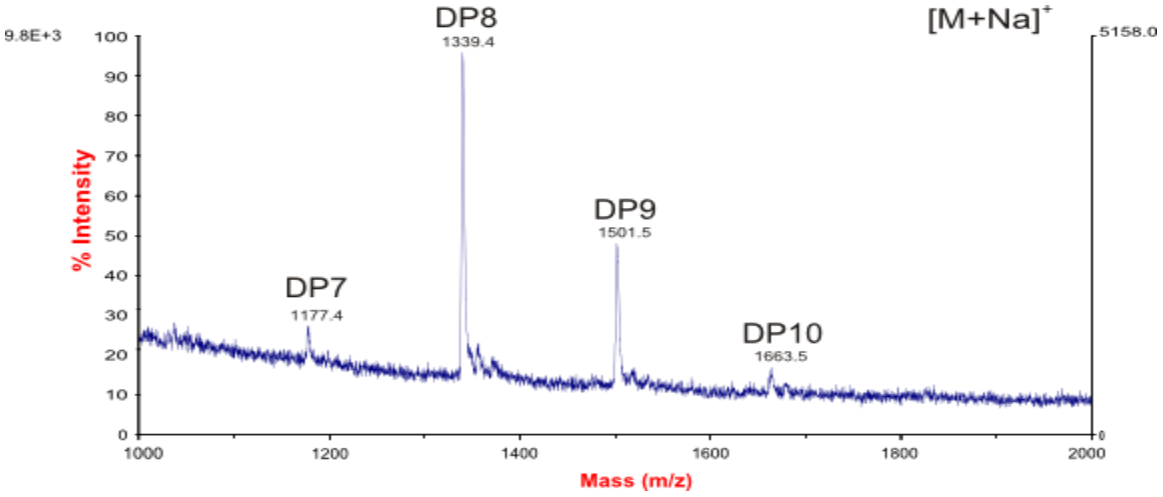

Figure 12 12. MALDI-TOF-MS graph of the products of a Glt 9 reaction with Laminarin DP6-ol as substrate.

3.1.5 NMR analyzes

3.1.5.1 Aldehyde results

In the 1D ^{1}H NMR spectra (**DP6**, **products**), anomeric signals (**Gi**, **Gt**, **G2**, **Gα**, **Gβ**) indicate the presence of β(1-3) linkages. The H-1 protons of the reducing-end glucose unit (**G1**) are at d 5.232 (H-1α), and d 4.672 (H-1β), respectively. The β-anomeric signal of the second glucose unit (**G2**) next to the reducing terminus is split into two doublets (d 4.759, H-1_α / d 4.776, H-1_β). The H-1 of the terminal

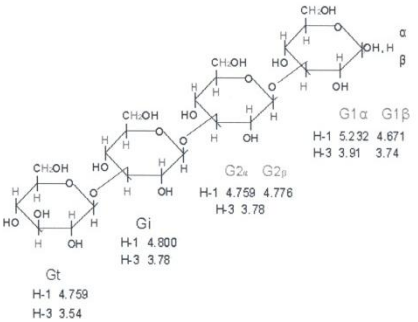

Figure 13. A The representative picture explains were Gi, Gt, G2, Gα and Gβ located. Picture curtesy of *Justina M. Dobruchowska*

glucose unit (**Gt**) is present at 4.759 and it is overlapping with H-1$_\alpha$ of the second glucose unit (**G2**). The doublet resonating at d 4.800 is stemming from the H-1s of the internal glucose units (**Gi**). The complete assignment of all protons is listed in table 2 in appendix. The NMR does not show any indication of the formation of β (1-6) linkages.

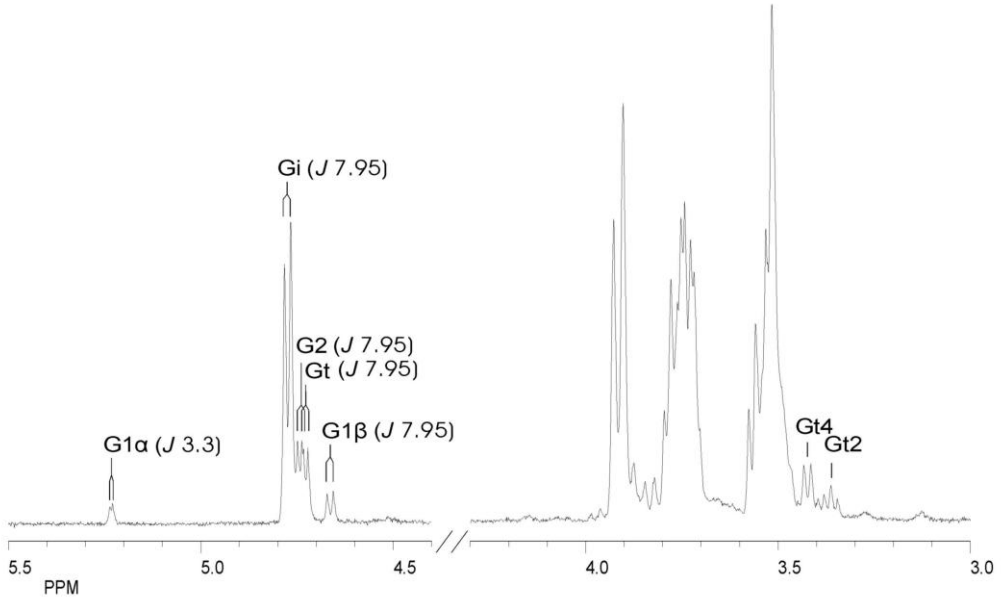

Figure 14. NMR graph of aldehyde product from the Glt 9 reaction with laminarin hexose.

3.1.5.2 Alditol NMR results

In the 1D ^{1}H NMR spectra (**DP6-ol**, **products**), anomeric signals (**Gi**, **Gt**, **G2**,) indicate the presence of β (1-3) linkages. The β-anomeric signal of the second glucose unit (**G2**) is split into two doublets (d 4.759, H-1$_\alpha$ / d 4.776, H-1$_\beta$). The H-1 of the terminal glucose unit (**Gt**) is present at 4.759 and it is overlapping with H-1$_\alpha$ of the second glucose unit (**G2**).. The complete assignment of all protons is listed in table 2 in appendix

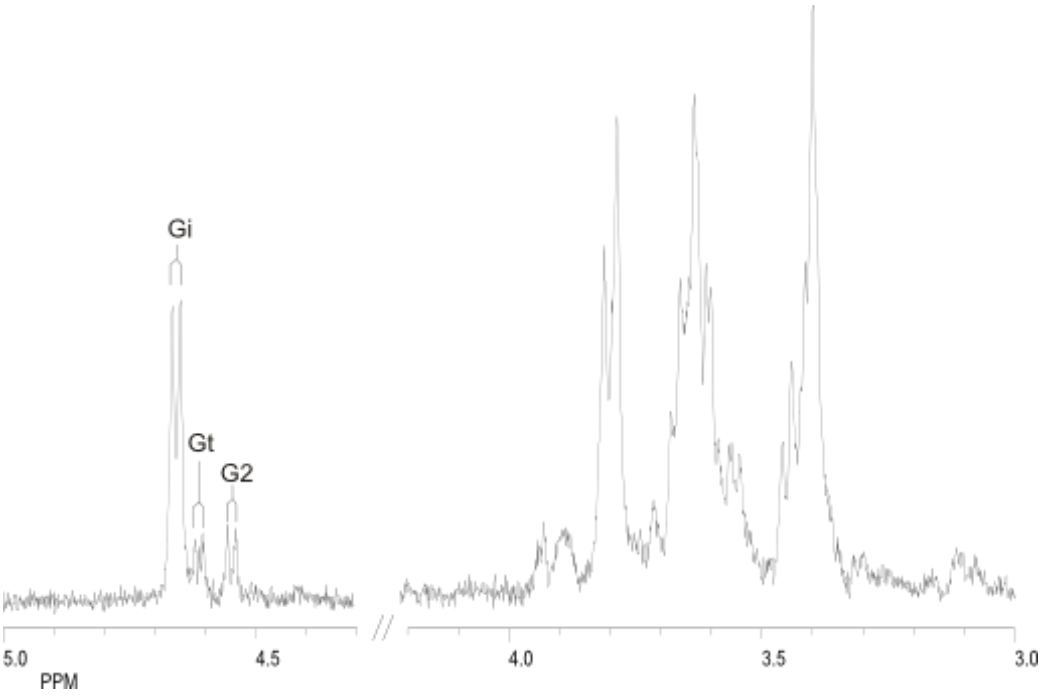

Figure 15. NMR graph of alditol product from the Glt 9 reaction with laminarin hexose.

3.1.6 Electrospray

Electrospray-ionization mass spectrometry (ESI-MS) was used to get more insight into the structures of the products formed from the substrates (DP5-ol and DP6-ol) by the Glt9 enzyme. It was shown by MALDI-TOF MS and NMR spectroscopy that many products are formed, differing in molecular masses (e.g. DP7-ol, MW=1154; DP8-ol, MW=1316; DP9-ol, MW=1478; etc.). But each product with one MW consists of different structures. However, these products were only available in mixtures, making structural analysis difficult. Using ESI-MS, it is possible to run a first spectrum (MS1) showing the complexity of a mixture by the molecular masses [M+Na]+ of the constituent compounds. One by one, these [M+Na]+-masses can be selected and the fragmentation can be studied by sequential Msn experiments. In order to get familiar with the fragmentation of (1-3)-gluco-oligosaccharide-alditols, DP8-ol and DP9-ol were first studied as linear free oligosaccharide-alditols, data not shown. Fragmentation, which started from the left or from the right side, can be discriminated because of the terminal reduced glucose residue (Glc-ol) on the right side. Purified fraction from the gel filtration on Bio-gel P2 of the reaction of Glt9 with DP6-ol was applied to the electrospray, and the DP7-ol peak was chosen and fragmented further.

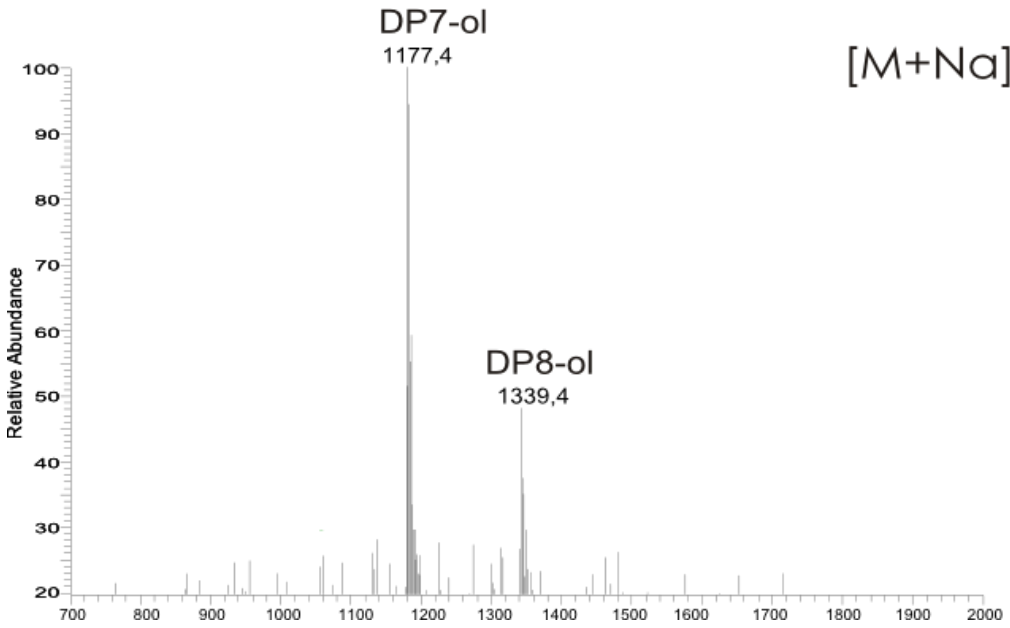

Figure 16. As can be seen on the graph a two peaks are formed at heptose and octose.

The DP7-ol peak was chosen and fragmented further to look at the pattern.

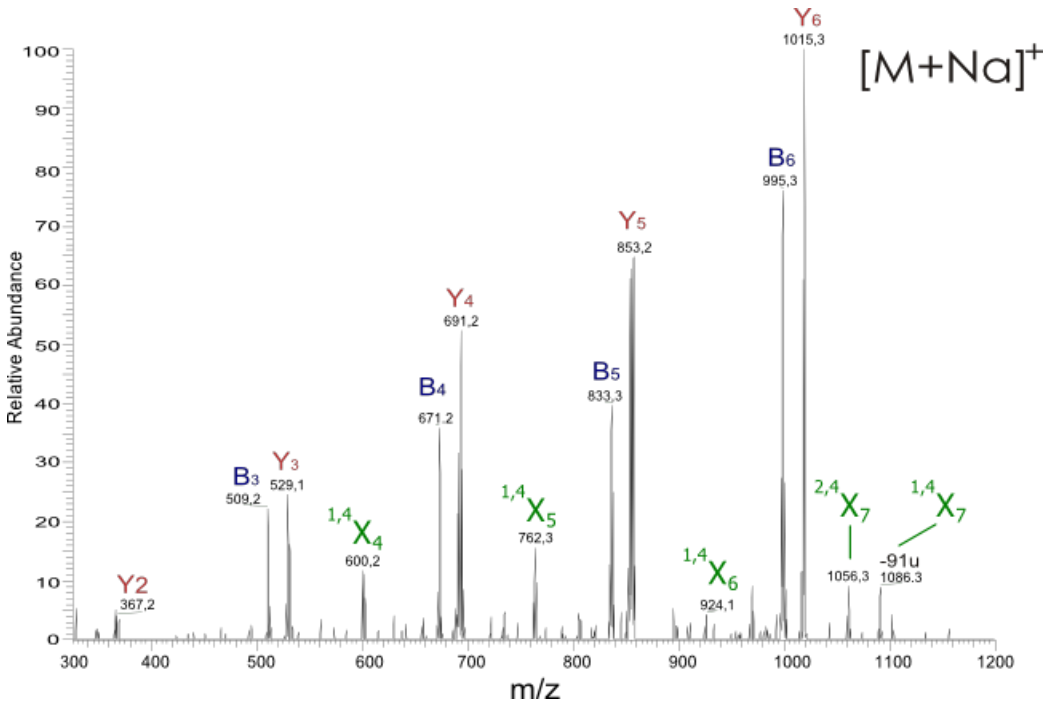

Figure 17. The figure shows how the peak DP7-ol is fragmented into smaller peaks. The peak Y6 at 1015,3m/z is from the cleavage of one glucose unit from alditol end. The peak Y5 at 852,2m/z is breakage of two glucose units from non-reducing end. The peak Y4 691,2m/z is breakage of three glucose units from nonreducing end. The peak Y3 at 529,1 m/z is breakage of 4 glucose units from the non-reducing end. The peak Y2 at 367,2 m/z is breakage of 5 glucose units from the non-reducing end. The peaks marked B3 to B5 is similar breakage of the glucose units except the breakage is from the reducing end. The smaller peaks in-between are the results from breakage of the glucose ring marked with X in Figure 18,

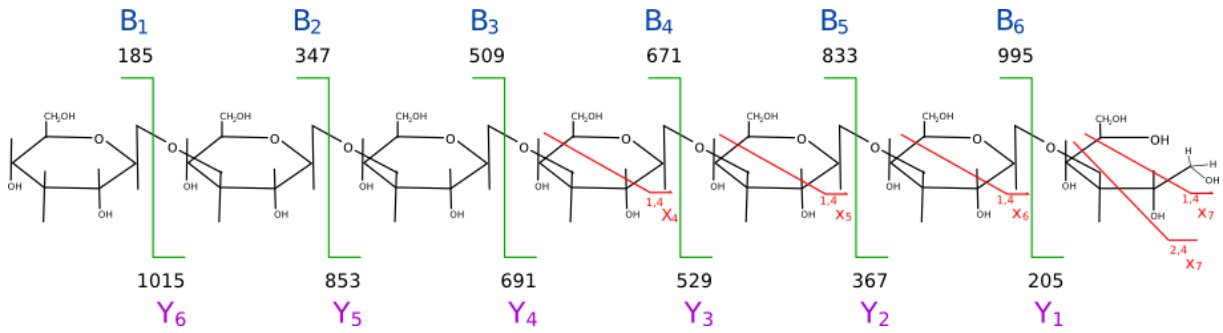

Figure 18. The figure shows how the peaks are formed. It is a breakage in the β (1-3) linkage that can explain the all the fragmented peaks we see at Figure *17*

From Figure 17 of the electrospray cleavage of the product DP7-ol it becomes clear that the product is only comprised of β (1-3) linkage type. The peaks marked with Y can only be explained by the cleavage of the β (1-3) linkage from the alditol end. The peaks marked with B are cleavage from the non-reducing end of the oligosaccharide. The different size of the peaks can be explained by looking at the alditol end but is changes the Mw of the oligosaccharide and is predominant in the graph. Also visible are intra breakages inside the glucose molecule which is marked with X in Figure 18. The cleavage pattern is shown in Figure 18. These beaks are not as predominant as the other two types. As there are no other peaks visible that would indicate that only linkage type found in the product is β(1-3)

3.1.7 Glt9 - Summarized results

According to the analytical results described above, Glt9 cuts the laminarin chain of size n from the non-reducing end forming mainly a single glucose unit (dp1) which is then added to another laminarin chain forming a product of size dp n+1.

3.2 Glt13 from *Rhodopseudomonas palustris*

3.2.1 Cloning and expression of *glt13*

The amplification of the DNA sequence gave a strong and visible band on a agarose gel and the size the amplified DNA was correct (data not shown). The expected size for *glt9* clone was 876bp. The gene was successfully cloned into pJOE3075 and following expression cultivation a strong band was detected on SDS gel (data not shown).

3.2.2 Purification of Glt13

Supernatant from cell disruption was collected after sonification and filtrated through 0.45µm filter before a 1mL of supernatant was loaded onto 5mL amylose column. Flow through and peaks from the column were collected into tubes with a fraction collector. Peak fraction from A3 to A8 were collected together and 1,5mL of that solution was desalted through 5mL desalting column in ULP buffer. Peaks

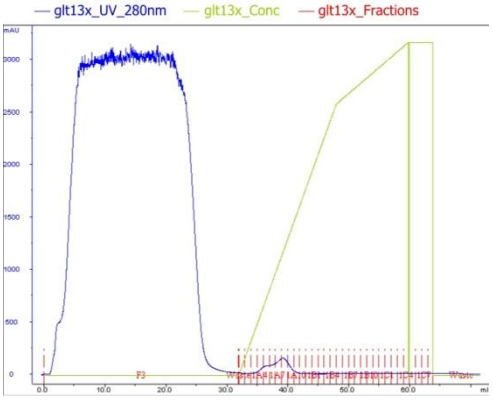

Figure 19 Show a graph of amylose purification. The sample is eluted in fractions A3 to A7

from the desalting column was pulled together, 200µL from the desalted column was added to 20µL 0,1mg/mL ULP protease, reaction was done at 30°C and 480rpm overnight. Figure 18 shows the purification profile of Glt13 on the amylose column. Following purification, the fusion protein was incubated with Ulp1 protease, which cleave the MalE domain from the GH17 Glt13 domain (data not shown). The enzyme domain was separated from the MalE domain by running the digestion products on a his column which immobilized the MalE domain. The purified enzyme was used in subsequent enzyme reactions.

3.2.3 TLC of reaction products

In Ficture 20, the substrate and products for the reaction of Glt13 with laminarin hexose for 3 days is visible. The prominent band is the laminarin hexose which is the substrate. After the reaction the products were purified on Biogel P2 column, larger products were examined with NMR and Maldi TOF. By looking at the TLC at lane D it is clear the enzyme is producing a bigger oligo saccharide and the size is at least one glucose unit bigger (DP7). Also there is a visible a smaller oligo saccharide which is also one glucose unit shorter (DP5). Also faintly visible are a larger oligosaccharide which appears to be two glucose units bigger (DP8) and two glucose units smaller (DP4).

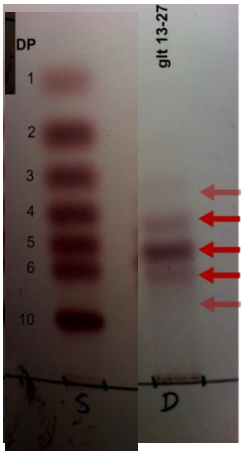

Ficture 20 Show the reaction of glt 13 in lane D with laminarin hexose. The arrows point to the substrate (middle) and products.

3.2.4 Maldi TOF

3.2.4.1 Aldehyde

MALDI-TOF-MS analysis of DP6 products revealed a major [M+Na]+ peaks at m/z 1029.5 and 1175.3, corresponding with Hex6 and Hex7. Three minor [M+Na]+ peaks at m/z867.5, 1353.6 and 1515.7 corresponding with Hex5, Hex8 and Hex9, but it not clear at this stage what linkage type there are involved.

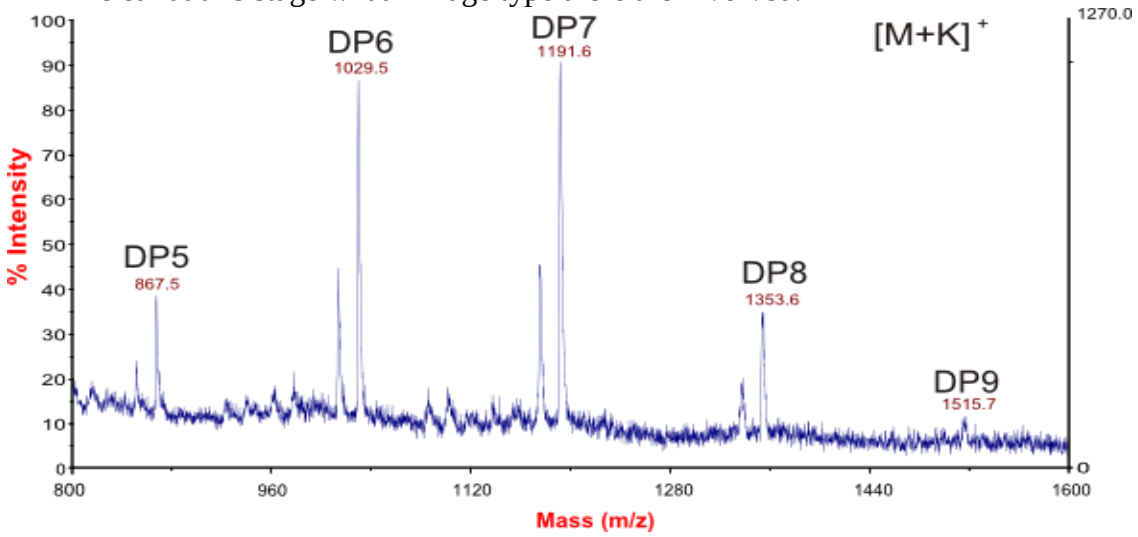

Figure 21. Maldi-TOF spectra of products from the reaction of Glt13 with laminarin hexose.

3.2.4.2 Alditol

MALDI-TOF-MS analysis of DP6-ol products revealed a major [M+Na]+ peak at m/z 1177.4, corresponding with Hex7 and two minor [M+Na]+ peaks at m/z, 1015.4and 1339.4 corresponding with Hex6 and Hex8

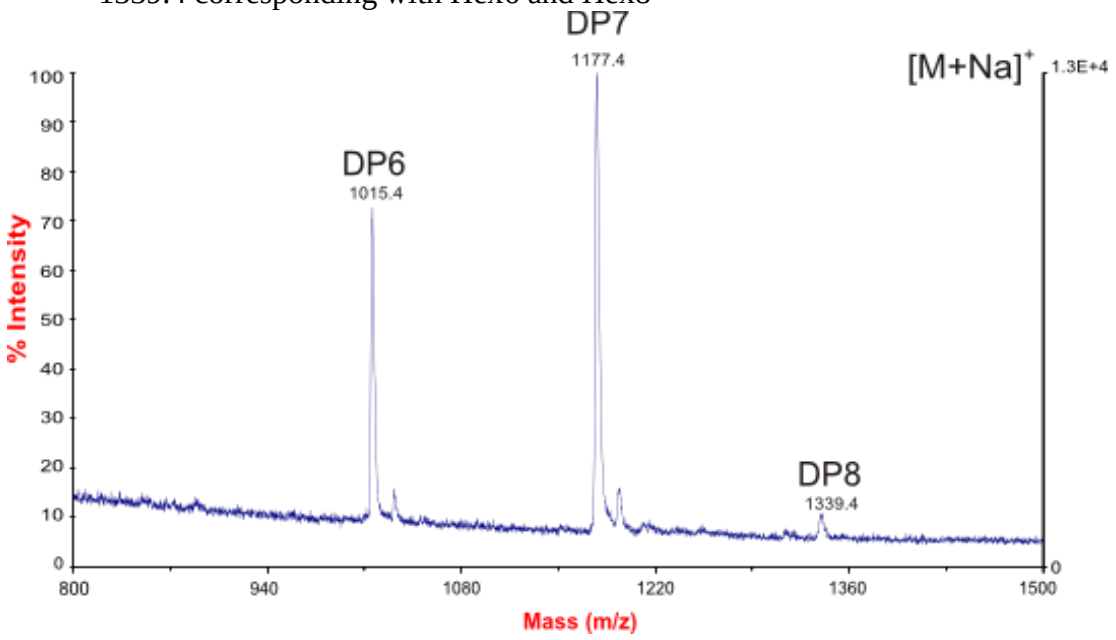

Figure 22. Maldi-TOF spectra of products from the reaction of Glt13 with laminarin hexose.

3.2.5 NMR

3.2.5.1 Aldehyde

In the 1D 1H NMR spectra (DP6, products), anomeric signals (Gi, Gt, G2, Gα, Gβ) indicate the presence of (β1-3) linkages. The H-1 protons of the reducing-end glucose unit (G1) are at d 5.232 (H-1α), and d 4.672 (H-1β), respectively. The β-anomeric signal of the second glucose unit (G2) next to the reducing terminus is split into two doublets (d 4.759, H-1α / d 4.776, H-1β). The H-1 of the terminal glucose unit (Gt) is present at 4.759 and it is overlapping with H-1α of the second glucose unit (G2). The doublet resonating at d 4.800 is stemming from the H-1s of the internal glucose units (Gi). The complete assignment of all protons is listed in Table 2 in appendix

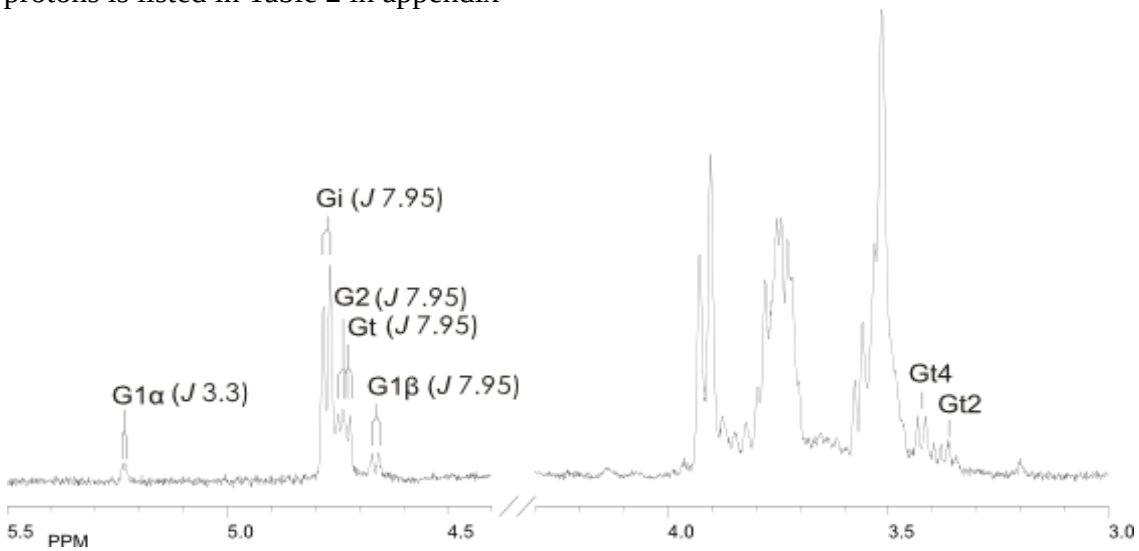

Figure 23. NMR graph of aldehyde product from the Glt13 reaction with laminarin hexose.

3.2.5.2 Alditol

In the 1D 1H NMR spectra (DP6-ol, products), anomeric signals (Gi, Gt, G2,) indicate the presence of β (1-3) linkages. The β-anomeric signal of the second glucose unit (G2) is split into two doublets (d 4.759, H-1α / d 4.776, H-1β). The H-1 of the terminal glucose unit (Gt) is present at 4.759 and it is overlapping with H-1α of the second glucose unit (G2). The complete assignment of all protons is listed in Table 2 in appendix.

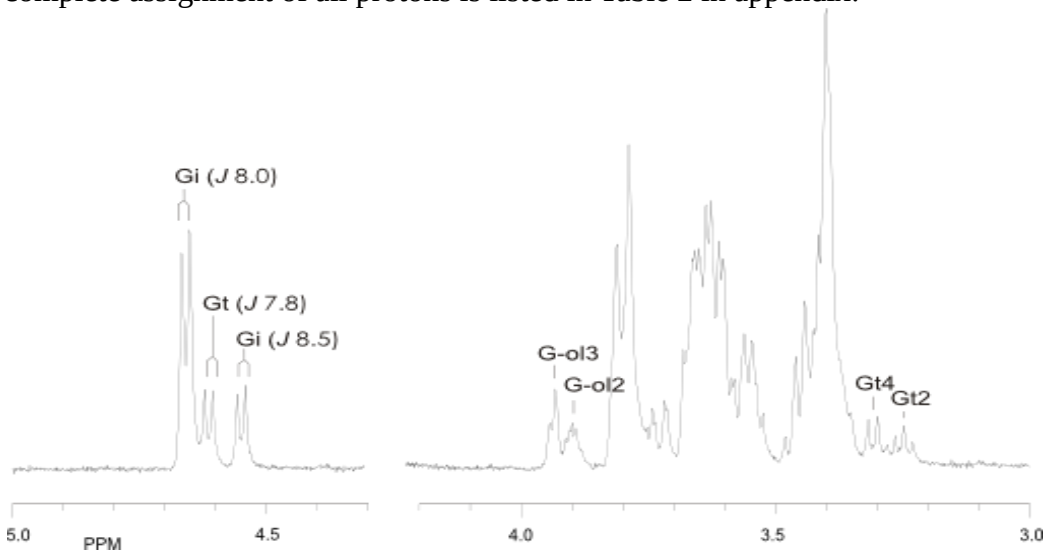

Figure 24. NMR graph of alditol product from the glt 13 reaction with laminarin hexose.

3.2.6 Glt13 - Summarized results

Although the analytical results did not include results from Electrospray-ionization mass spectrometry (ESI-MS), the results clearly indicate that Glt13 cuts the laminarin chain (of size n) from the non-reducing end forming mainly a single glucose unit (dp1) which is then added to another laminarin chain forming a product of size dp n+1 similar as Glt9.

3.3 Glt 20 from *Bradyrhizobium japonicum*

3.3.1 Cloning and expression of *glt20*

The amplification of the DNA sequence gave a strong and visible band on an agarose gel and the size of the amplified DNA was correct (~880 bp). The gene was successfully cloned into pJOE4095. Following cultivation, the yield of expression was examined by running cell crude extracts on SDS gels (figure 25).

From the SDS gel it is clear that the expression was good. The recombinant fusion protein consisted of a 31,5kDa GH17 domain and a 56kDa MalE domain. The recombinant enzyme of size 87,8kDa in the crude extract of the production clone is seen in lane2, Figure 25. The expression is around 20% of the total protein by visual inspection of the gel. So the expression of the enzyme was considered successful.

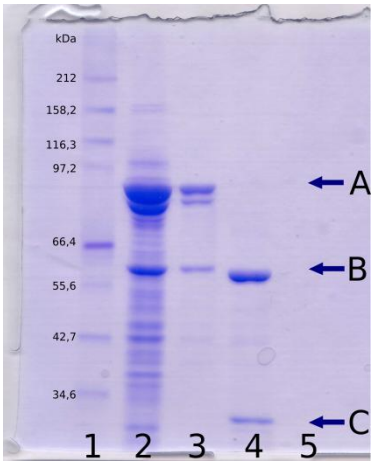

Figure 25. 10% SDS gel of Glt20 crude extract and purification fractions. (1) Protein standard. (2) Sample on amylose column. (3) Sample after amylose column. (4) Sample after ULP reaction. The arrows point to the following bands: (A) Enzyme with MalE domain. (B) MalE domain. (C) GH17 Enzyme Glt 20

3.3.2 Purification

After cultivation then the cells were spun down, dissolved in amylose buffer and erupted in sonicator. After eruption the supernatant was spun down from the pellet in a Eppendorf counter centrifuge for 5minutes at 13.200 rpm and 4°C.
Supernatant from cell eruption was collected after sonification and filtrated through 0.45µm filter before a 1mL of supernatant was loaded onto 5mL amylose column. Flow through and peaks from the column were collected into tubes with a fraction collector.
Peak fractions from A3 to A8 were collected together and 1.5mL of that solution was desalted through 5mL desalting column in ULP buffer. Peaks from the desalting column were pulled together.
200µL from the desalted column was added to 20 µL of 0,1mg/mL ULP protease. Reaction was done at 30°C and 480rpm over night.
Following digestion, a sample was run on a SDS gel (Figure 25).

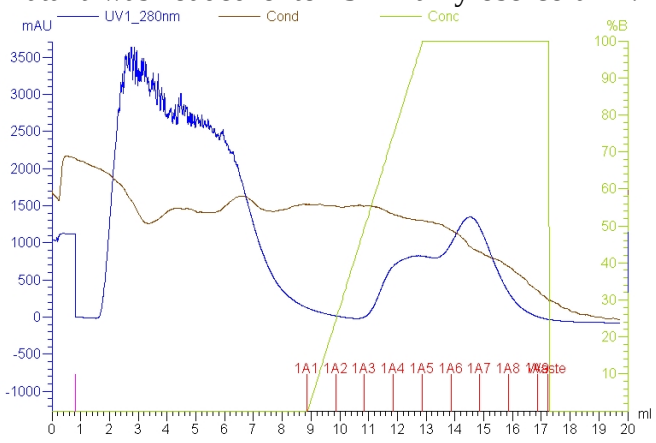

Figure 26 Show a graph of amylose purification. The sample is eluted in fractions A3 to A8

Degradation products of the Ulp1 protease can be seen on the gel, i.e. the GH17 domain (31,5 kDa) and the MalE domain (56 kDa). The GH17 domain was separated from the MalE domain by running the sample containing the digestion products on a His column (Nickel). The MalE with a His tail was immobilized on the column whereas the GH17 ran through. Purified enzyme was used in subsequent enzymes reactions.

3.3.3. Substrate specification - TLC

Purified enzyme was routinely tested at 30°C on DP3 to DP7 for 3 days. The reaction progress was monitored by spotting the reaction on TLC. The reaction was as follows:

10µL 6.25mg/mL Substrate curdlan DP3 to DP7
3µL 0.5M KPO4 pH 6.5
7µL 0.72mg/mL Purified enzyme

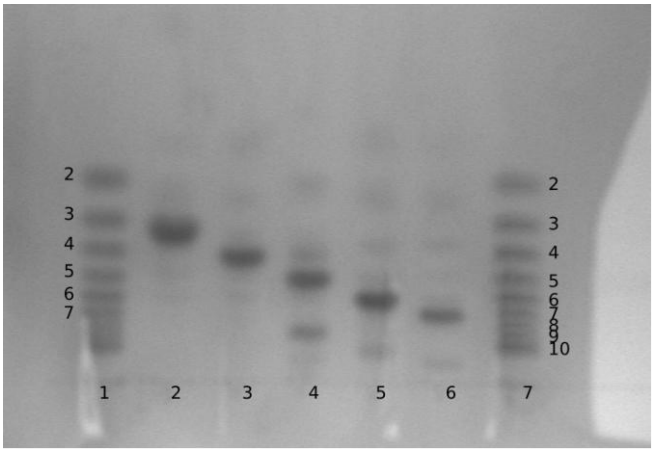

Figure 27. The figure shows the products from the reaction of Glt 20 with β-glucan substrates of diffrent length. Lane 1 is oligo standard from 2 to 10, lane 2 is triose, lane 3 is tetrose, lane 4 is pentose, lane 5 is hexose lane 6 is heptose and lane 7 is an oligo standard from 2 to 10. For the substrates of DP5, 6 and 7, products of DP8, 10 and 12 is formed. This indicates that the enzyme is cutting from the reducing end and tranfering the remaining saccharide with new reducing end to the acceptor molecule.

As can be seen in Figure 27 the transferase reaction is efficient when the size of the substrate is at least DP5. Still, there is evidence of transferase activity at lower oligosaccharides e.g. DP 4. The

enzyme is producing a larger oligo saccharide which is clearly visible from DP 5 and upward. Smaller oligosaccharides are also produced, which are a by-product of the transferase reaction.

3.3.4 Purification of saccharide products

The products from the reaction were purified on bio-gel p2 column. The entire sample was loaded onto the column and fractions from the column were collected after 2 hours in Eppendorf tubes. The fractions were collected at 5 minutes interval.

The fractions that were pure were pulled together, freeze dried and analysed on Maldi TOF and NMR. In this instance, fractions from 6 to 9 were pulled together.

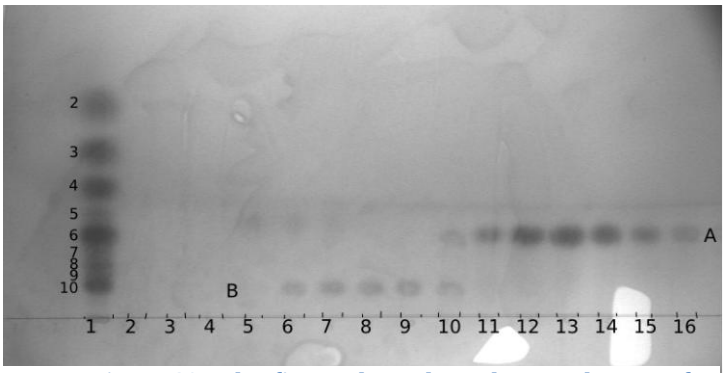

Figure 28. The figure shows how the sample was after purification on bio-gel P2. As seen there was a good seperation of the products from the substarate. Lane: (1) Standard DP2 to 10. Lanes 2-16) Fraction 1 to fraction 16. Line A: DP6. Line B: Tranferease products for analyses.

3.3.5 MALDI-TOF-MS

MALDI-TOF-MS analysis of the reaction before the purification of product was done revealed two peaks at m/z 1175,3 and 1191,3. These peaks are the substrate DP 7 with two different types of ions Na^+ and K^+. Second largest peaks are at m/z 1985.5 and 2025.5 this is the product formed DP 12. There are also visible another peaks at DP5, DP6, DP8, DP10 and DP11 in lower intensity highest is 22. The product formed is approximately 30% of the substrate.

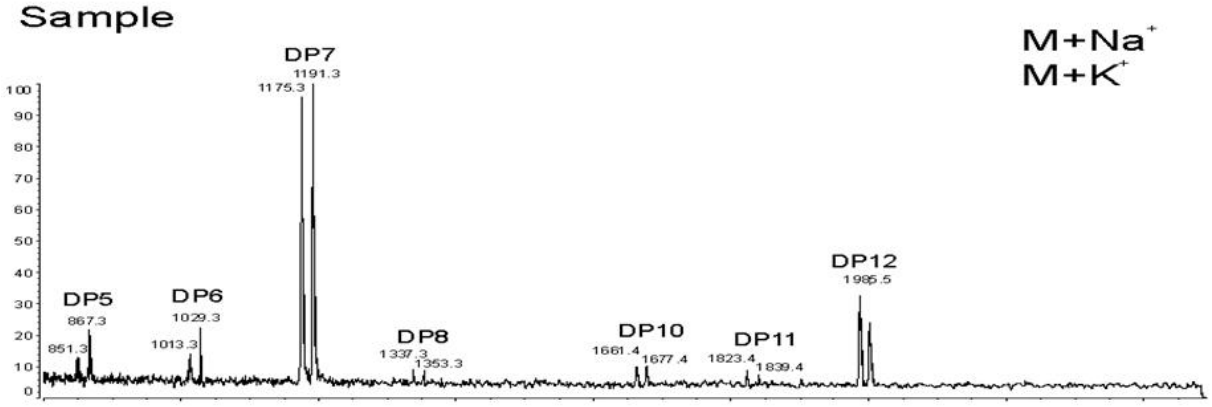

Figure 29. Maldi TOF of the Glt20 reaction products with the substrate laminarin DP7, before purification on Bio-gel P2 column.

MALDI-TOF-MS analysis of DP5 products revealed a major [M+Na]+ peak at m/z 1337.2, corresponding with Hex8 and three minor [M+Na]+ peaks at m/z 1175.1, 1499.2 and 1661.3 corresponding with Hex7, Hex9 and Hex10, respectively

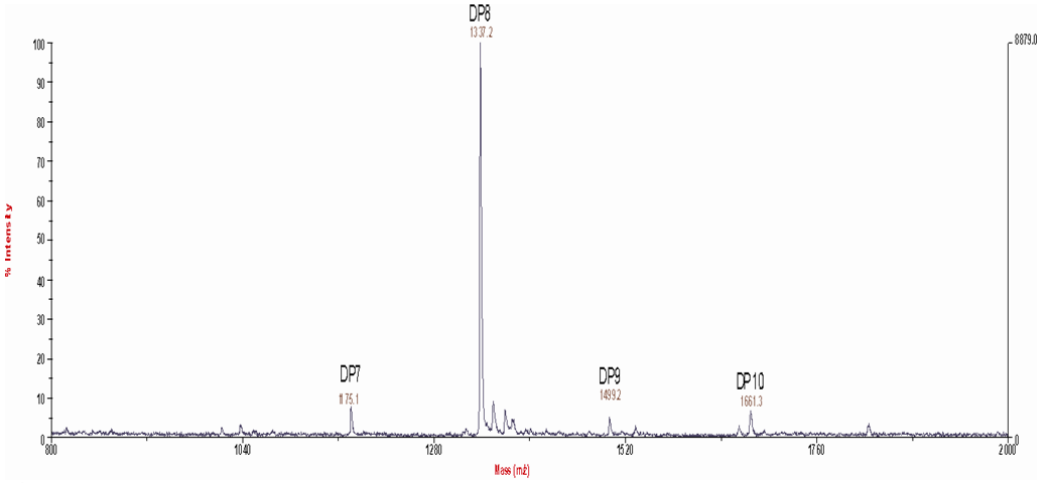

Figure 30. Maldi TOF graph of the product of laminarin pentose reaction of Glt 20

The MALDI-TOF mass spectrum of **DP6 products** revealed $[M+Na]^+$ a major peak at *m/z* 1661.3 corresponding with Hex_{10} and a minor peak corresponding with 1499.2 ,

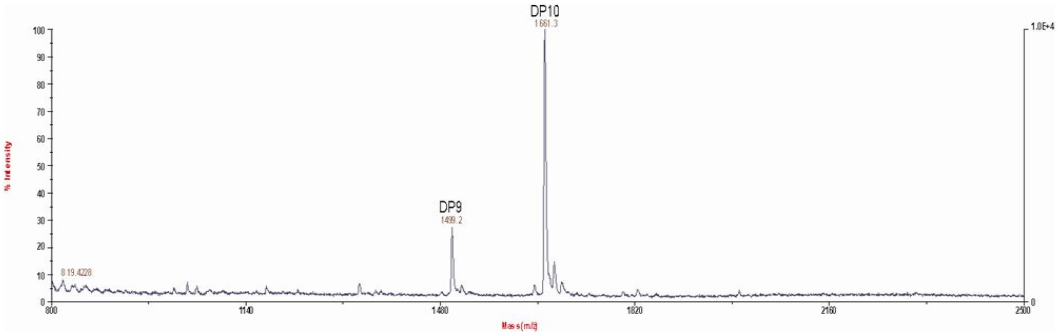

and Hex_9.

Figure 31. Maldi TOF picture of the product of laminarin hexose reaction of Glt20. Major product is of size DP10

MALDI-TOF-MS analysis of DP7 products revealed a major [M+Na]+ peak at m/z 1985.0, corresponding with Hex12 and three minor [M+Na]+ peaks at m/z 1661.0, 1823þ0 and 2147.1 corresponding with Hex10, Hex11 and Hex13, respectively

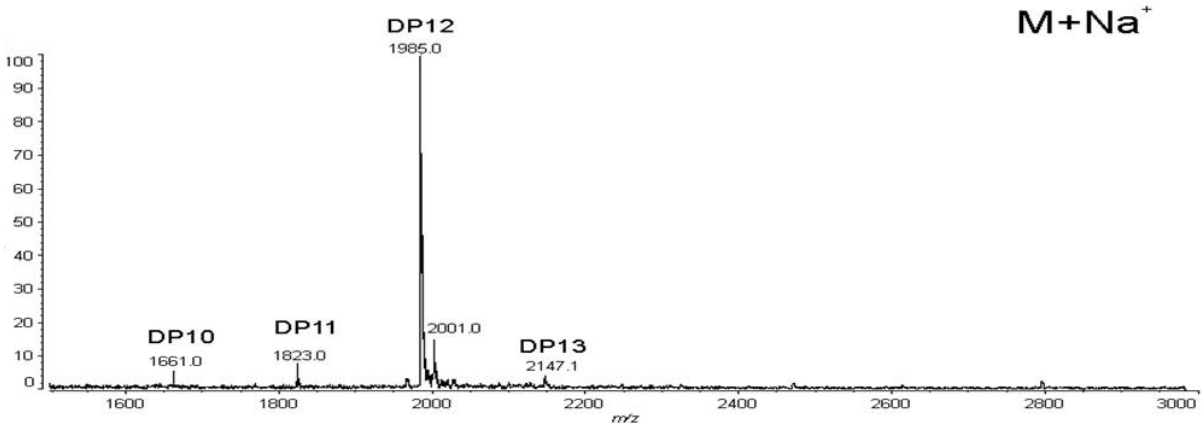

Figure 32 Maldi TOF picture of the product of laminarin heptose reaction of Glt20. Major product is of size DP12

3.3.6 NMR

In the 1D ^{1}H NMR spectra (**DP5**, **DP6**, **products**), anomeric signals (**Gi**, **Gt**, **G2**, **Gα**, **Gβ**) indicate the presence of β (1-3) linkages. The H-1 protons of the reducing-end glucose unit (**G1**) are at d 5.232 (H-1α), and d 4.672 (H-1β), respectively. The β-anomeric signal of the second glucose unit (**G2**) next to the reducing terminus is split into two doublets (d 4.759, H-1$_{\alpha}$ / d 4.776, H-1$_{\beta}$). The H-1 of the terminal glucose unit (**Gt**) is present at 4.759 and it is overlapping with H-1$_{\alpha}$ of the second glucose unit (**G2**). The doublet resonating at d 4.800 is stemming from the H-1s of the internal glucose units (**Gi**). The complete assignment of all protons is listed in Table 2

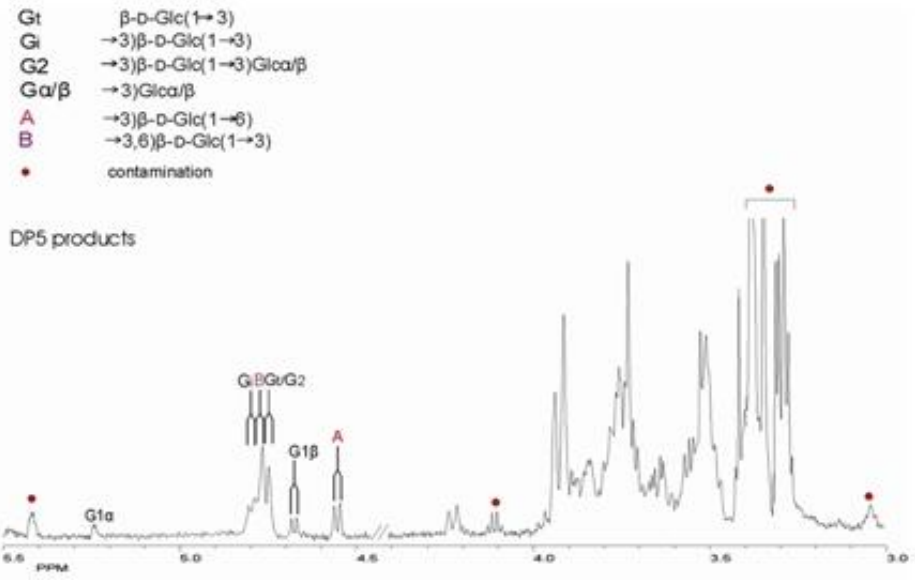

Figure 33. NMR spectra of the laminarin pentose product DP 10

Two anomeric signals (**A**, **B**) observed at δ 4.56, and δ 4.75, together with a doublet signal at δ 4.22 indicate the presence of β(1-6) linkages. The residue **A** is identified as a [→3)Glc(1→6)]. Residue **B** (overlapping with **Gi**, **Gt**, **G2**) can be identified as [→3,6)-β-D-Glc-(1→3)] glucose unit. The ^{1}H chemical shifts of the residues (**A**, **B**)

should be confirmed by means of 2D NMR spectroscopy (TOCSY). There is a possibility that instead of branching, an internal [→6)-β-D-Glc-(1→3)] glucose unit is present.

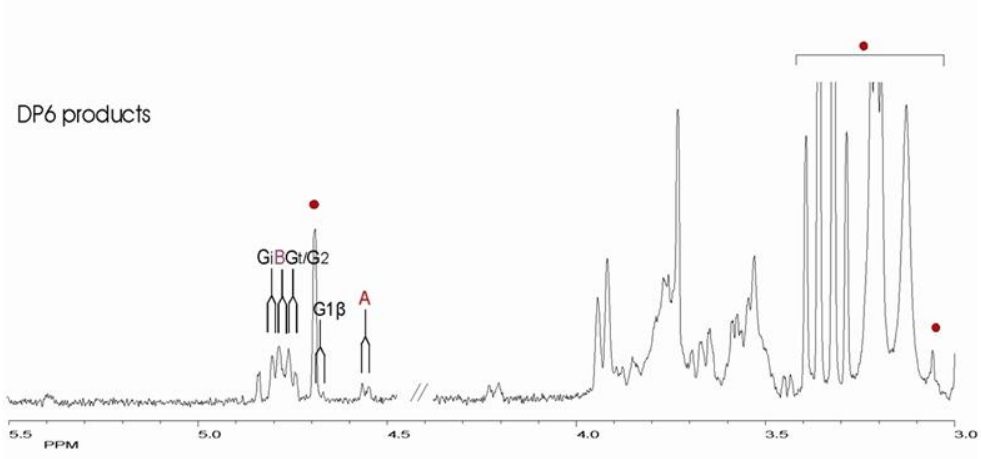

Figure 34 NMR spectra of the laminarin hexose product DP 12

It is clear by examining the two NMR spectra that β(1-6) linkages are formed in the reaction of Glt20 with laminarin pentose and hexose. This is supported by comparing these results with known retention time and coupling constant of standards, see Table 2.

Also by comparing the results from the NMR with known disaccharides see Table 1 it is supported that β(1-6) linkages are produced.

Table 1. ^{1}H-NMR chemical shifts[a] of β-D-gluco-disaccharides recorded in D_2O at 292K for sophorose and laminaribiose, and at 300K for cellobiose and gentiabiose. Coupling constants (Hz) are given between brackets.

Disaccharide		Anomeric protons		Glycosidic proton	
		H-1α	H-1β	H-1	
				H-1$_\alpha$	H-1$_\beta$
Sophorose	(β1-2)	5.447 (3.0)	4.789 (7.3)	4.623 (7.3) / 4.717 (7.3)	
Laminaribiose	(β1-3)	5.232 (3.6)	4.673 (8.5)	4.719 (8.5) / 4.736 (8.5)	
Cellobiose	(β1-4)	5.232 (3.6)	4.669 (7.9)	4.520 (7.9)	
Gentabiose	(β1-6)	5.234 (3.6)	4.660 (8.5)	4.501 (8.5) / 4.518 (8.5)	

[a]In ppm relative to the signal of internal acetone (δ 2.225)

3.3.7 Glt20 - Summarized results

According to the analytical results described above, Glt20 cuts the laminarin chain from the reducing and transfer the chain with the new reducing end (donor) to another laminarin chain (acceptor) forming 1,6 linkage. The data does not reveal if a branch or

an elongation with a 1,6 linkage is formed.

4 Discussion

4.1 Comparison of DNA sequence

Structural differences between Type I and Type II bacterial enzymes

The work described in this master thesis involved cloning and expression of genes encoding GH17 domains from three different Proteobacteria species. Furthermore, the activity of the enzymes was characterized using laminarin oligosaccharides as substrate. A previous work carried out at Matís-Prokaria and the University of Utrecht revealed that GH17 domains found in such bacteria exhibit a non-Leloir trans-β-glucosylation activity.

A part of this work involved a sequence-structure analysis of Type I and Type II enzymes was done to identify structural features that are conserved only within one group and thus distinguishing between them. The analysis was primarily aimed at finding features that might explain different substrate specificity, i.e. in potential substrate binding regions. The structural analysis with reference to alignment indicated three regions around the substrate binding-cleft, which seem unique for type II sequences. Figure 35 shows a part of the alignment including two of these regions. In these regions, unique acidic residues are found and the third region contains a basic Arginine residue. These residues seem unique for Type II domains and line the substrate-binding cleft of the domain. These specific regions may thus possibly be involved in substrate binding and contribute to different substrate specificity.

Taking this into consideration, two Type II enzymes were selected for a further examination in this project along with the Type I enzyme NdvB from *Bradyrhizobium japonicum*, which in this work was designated Glt20.

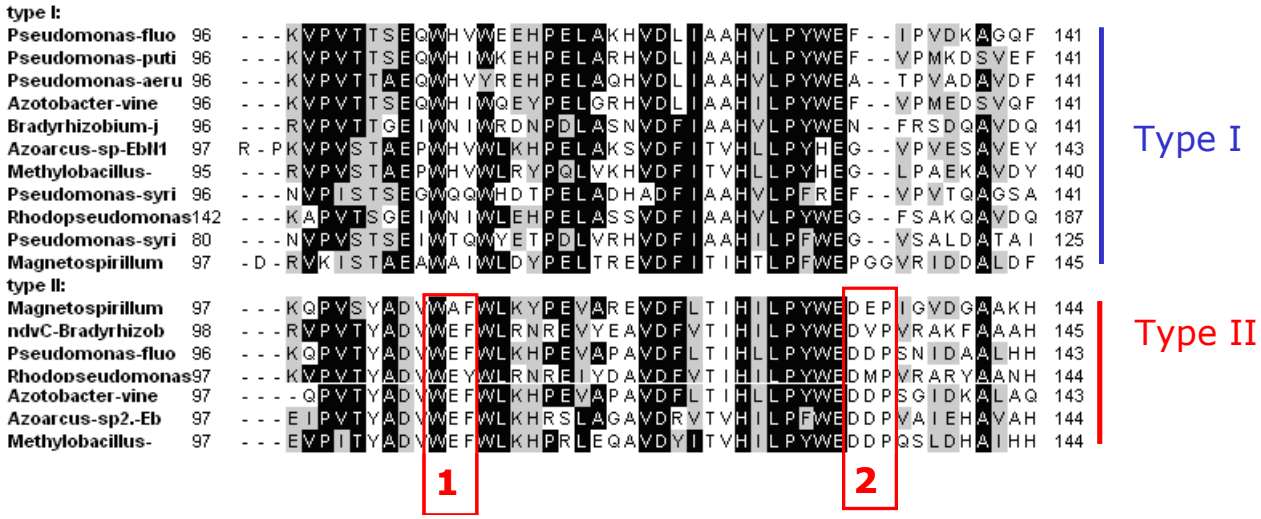

Figure 35 Amino acid sequence alignment of GH17 type I and type II enzymes. Only part of the overall alignment is shown which includes two regions around the substrate binding cleft site.

4.2 Expression and Column purification

Research has shown that MalE can increase the expression of proteins by 65% (Pryor et al., 1997) (Terpe, 2003). MalE can also have another effect to increase the solubility of proteins. Another type of expression system could produce the same amount of proteins at the expense of the solubility. (Pryor et al., 1997)

A downside to adding a large Mal E domain to the cloned enzyme is that the MalE domain can have a steric hindrance effect blocking the active site of the enzyme. With the cloning vector pJOE4901 a linker, Smt3 with His tag is inserted between the MalE domain and our cloned enzyme. A special protease Ulp 1 recognises the Smt3 linker between the domains and hydrolysis it. As the protease and the MalE domain both have a his tag it is easy to purify them on a His Tag column but the cleaved enzyme does not bind to the column. (Pryor et al., 1997)

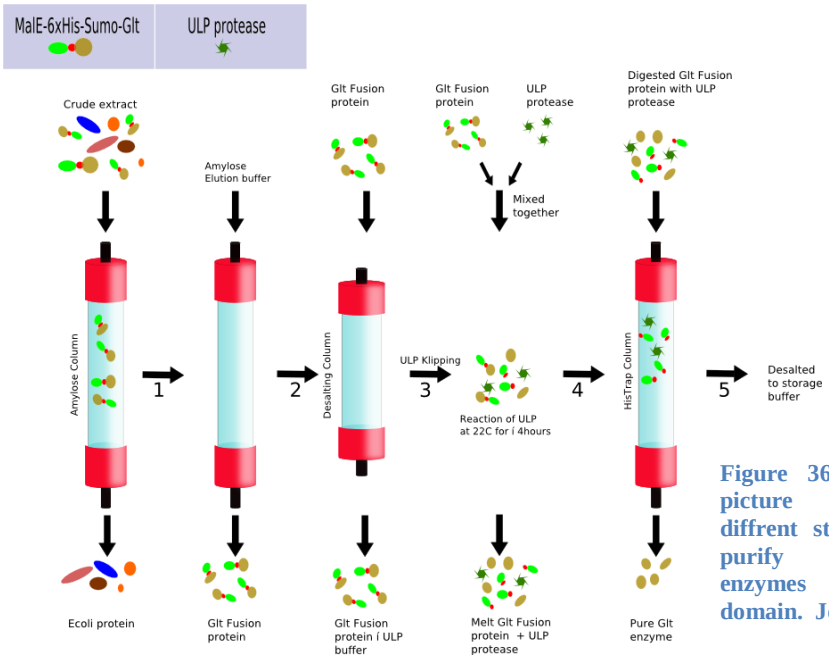

Figure 36 A schematic picture showing the diffrent steps needed to purify the cloned enzymes with Mal E domain. Jón Óskar

As the purification were carried out by affinity columns the reproducibility and scale up for these type of cloned enzymes was easy. The end product was very pure >99% as the enzyme was purified with two affinity columns. The only downside was the apparent degradation of some of the cloned enzyme and MalE domain after cultivation. This did not pose any problems except that the recovery of the cloned enzyme was slightly lower than expected after purification .

In the previous work of Hreggvidsson et al (2010) several expression systems were tested for the production of GH17 enzyme domains. The system giving the highest yield of active recombinant proteins was based on a MalE fusion. The same was observed for the cloning of the three different enzymes Glt 9,glt 13 and Glt 20 described in this work. The reason for improved expression with MalE could be related to the fact that only one domain of two of the natural occurring enzyme was cloned.

4.3 Glt 9

The production and the purification of the enzyme was successful. From the TLC data it is clear that the enzyme can use a DP 6 and DP 6-ol as a substrate and the major products are one glucose unit bigger and one glucose unit smaller than the substrate. The Maldi TOF confirms these results as there are visible peaks at the relative sizes. Also the intensity of the peaks indicates that the one glucose unit product is formed first. After longer incubation bigger oligo saccharides become visible as the enzyme can use the bigger oligo saccharide as a acceptors. The data from NMR and Electrospray experiments indicates that the linkage formed is β (1-3) as there are no visible peaks in NMR for β (1-6) linkages. Also Electrospray studies supports this as the cleavage pattern of the Dp7-ol can only be explained if the linkage type is β (1-3) (Figure 17). Therefore it can be stated that glt 9 is not a branching enzyme but β (1-3) elongation enzyme.

4.4 Glt 13

The production and the purification of the enzyme was successful. It is clear from the TLC data that the enzyme can use both DP 6 and DP 6-ol as a substrate and the major product is one glucose unit larger and one glucose unit smaller than the substrate. The Maldi TOF confirms these results as there are visible peaks at the relative sizes. The intensity of the peaks indicates that the plus one glucose unit product is formed first. Also when the time progresses bigger oligo saccharides become visible as the enzyme can use the bigger oligo saccharide as a acceptors. The data from NMR indicates that the linkage formed is β (1-3), as there are no visible peaks in NMR indicating β (1-6) linkages. Therefore it can be stated that Glt13 is not a branching enzyme but β (1-3) elongation enzyme.

From the data of the Glt9 and Glt13 enzymes, it is clear that the enzymes produces β(1-3) linkage and not β(1-6) linkage. For formation of β(1-6) linkage, it would be expected to see two new peaks forming a duplet in the NMR graph at 4,65ppm and another at 7,75ppm. These two new peaks represent the linkage types -3) β-D-Glc(1-6) and -3,6) β-D-Glc(1,3). Also, according to comparison with NMR from Kim et al., 2000, see Figure 6, there is only one possible linkage type within the newly formed oligo saccharide or β(1-3).

The data from the electrospray also supports this conclusion. Even though electrospray was only done for Glt9 product from alditol, the cleavage pattern is very decisive as it does not indicate any other linkages type other than β(1-3).

As to determine from which end, the enzyme is cleaving it is proposed that the enzymes are cutting from the non-reducing end as this would explain why the oligo saccharide is growing by only one glucose unit.

4.5 Glt 20

The production of recombinant Glt20 and subsequent purification was successful. It is clear from the TLC data that the enzyme can use a DP 5, DP, 6, DP 7 and to some extent DP 4 as a substrate. The Maldi TOF supports this theory as there are visible peaks at the relative sizes. Also the intensity of the peaks indicate that following

cleavage of the substrate, two glucose units are released and the remaining oligo is then ligated into acceptor. The data from NMR indicates that the linkages forms is β (1-6) as there are visible peaks in NMR for β (1-6) linkages. Therefore it is stated that Glt20 is a branching enzyme that produces but β (1-6). It cleaves the substrate from the reducing end, releasing laminaribiose and ligates the retaining donor oligo saccharide to and acceptor molecule, thus increasing the size of the oligo by the following formula M+ (M-2)=P were as M is the mass of the donor and P is the mass of the product.

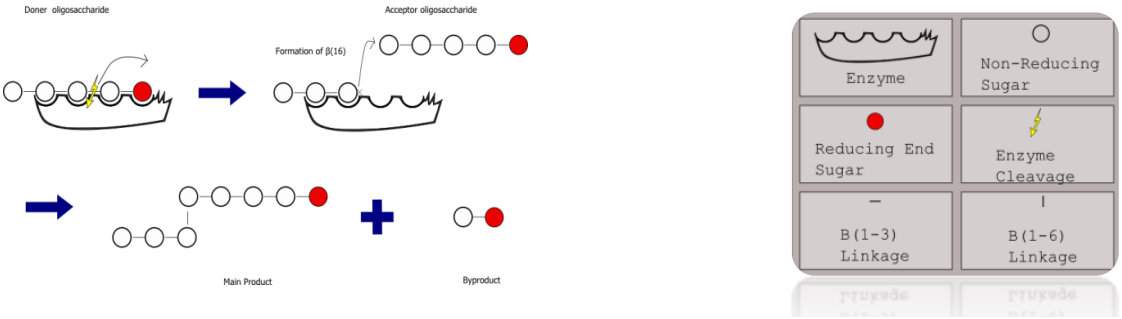

Figure 37. The figure shows a possible mode of the reaction of Glt 20 with the substrate DP 5. The enzyme strats by cutting the substrate from the reducing end and releasing laminarin biose. A secound DP5 enters the active site and the cut oligosaccharide is ligated with β(1-6) linkages. Thus forming a new link before releasing the new oligo saccharide. It is however not clear if the enzymes produces 1,6 branch or a kick as the figure indicates.

Glt20 cuts from the non-reducing end, which is different from the GH17 enzymes characterized so far from other bacteria in previous work. It is however in accordance with the findings of Gastebois et al., 2010 for AfBgt1p from the fungi *A. fumigatus* and Bgl2p of the yeast *S. cerevisiae*. These glucanosyltransferase catalyze the release of a laminaribiose unit from the reducing end of a substrate and transfer the newly generated reducing end to the non-reducing end of another β(1-3)glucan molecule, generating a new β(1-6) linkage. Figure 38 shows the possible products from the DP5 reaction:

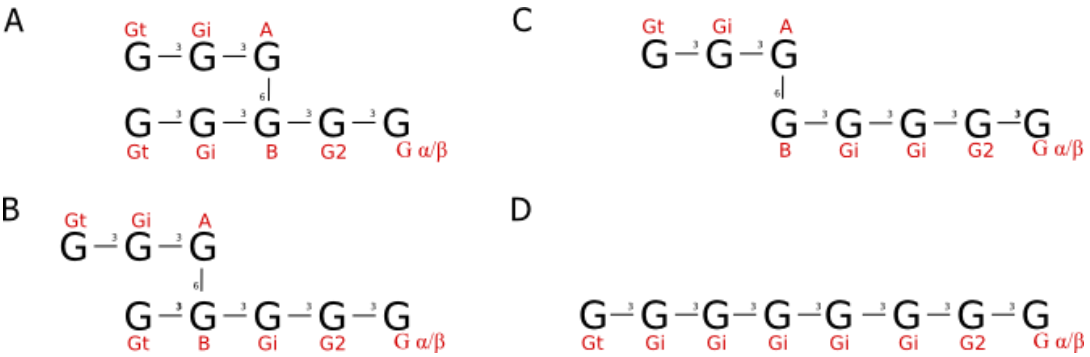

Figure 38. The figure shows how the reaction products for Glt 20 are possible. The most likely conformation is though the one that is a straight chain with a kink in it C. See better discussion in text

As the Glt20 enzyme is able to cleave the substrate from the reducing end, it should be able to produce cyclic molecules by transferring the new donor reducing to the non-reducing acceptor end of the same molecule, if the substrate β-glucan chain is long enough.

According to Bhagwat et al (1995), mutagenesis of *ndvB* from *Bradyrhizobium japonicum* resulted in hypoosmotically sensitive strain which was unable to synthesize cyclic β(1-3)β(1-6)glucans. Taking this into account and the results of this work, Glt20 or NdvB may be involved in formation of cyclic β-glucans by forming a β(1-6)

linkage between the newly formed reducing end and the non-reducing end of the same molecule. Thus, it would form a kick in the cyclic structure. The Glt20 GH17 domain probably works in synergy with the GT2 domain. According to the model set up in figure 1, the GT2 domain may be involved in the synthesis of the linear β-glucan chain.

Mutagenesis of *ndvC* from *Bradyrhizobium japonicum* resulted in a strain which produced predominantly β(1-3) linkages. This indicates that NdvC is involved in the synthesis of β(1-6) linkages. It is not clear if it adds branches to the cyclic structure or if it participates in modification of other linear β-glucans.

To study this further more substrate has to be used and also longer β-glucan chains as the cyclic reaction is only possible when the end of the saccharide is used as an acceptor.

The TLC data for the Glt20 reaction indicates also as for the previous enzymes that only about 10% of the substrate is converted to products. This is a problem for the study of the product as the substrate is still at 90% and it interferes with e.g. NMR. It is a time consuming work to produce and purify the product before further studies on them can be carried out.

For now there is no way to interpret where the new linkage is formed (kink or a branch), i.e., which product in figure 36 is the major product. Yet, according to the results of this work and the results of Bhagwat et al 1996, it is proposed that the new β(1-6) linkage is formed on the end of the new product .One way to establish the location of the linkage would be to use 2D TOCSY and/or electrospray.

The results do not explain the structural difference of type I and type II enzymes. It is clear that the type II enzymes Glt9 and Glt13 use β-glucan (laminarin, curdlan) as substrate and they resemble the previously characterized type I enzymes, Glt1, Glt3 and Glt7 (Hreggvidsson et al 2010) in the respect that they cleave a β-glucan chain from the non-reducing end and transfer the cleavage product with the new reducing end (donor) to the non-reducing end of an acceptor β-glucan chain. It is not clear where in the biological process in making complex OPG β-glucans the transfer takes place, which might explain the difference in type I and type II enzymes.

By studying the TLC data it becomes clear that the enzymes can only transform about 10% of the substrate into product. Even longer reaction time a depletion of substrate is not seen. It has been reported that a branching enzyme can behave as both hydrolase and transferase depending on the substrate concentration (Gastebois et al., 2010). To alleviate this problem a further future test could be done as to decrease the concentration of product form by e.g. gel filtration as to push the reaction towards the product.

5 Acknowledgements

I wish to express my gratitude to those who have helped me with this work.
First off I wish to thank my supervisor Dr. Guðmundur Óli Hreggviðsson and Dr. Ólafur H. Friðjónsson for their great support and good advice while working on these enzymes. I also what to thank Prof. Dr. Johannis Kammerling, Dr. Gerrit J. Gerwig

and Dr. Justina M. Dobruchowska from the University in Utrecht in Holland for all their help in lab in Holland and sharing her great insight into the world of oligosaccharides and their detection with NMR, Maldi-TOF and electrospray. I want also thank Sólveig Ólafsdóttir for all her support and help in the lab at Prokaria. Finally, I am grateful to my family, especially to my wife María for all her help and support during these studies.

6. Appendix

DNA Ladder from New England Biolabs

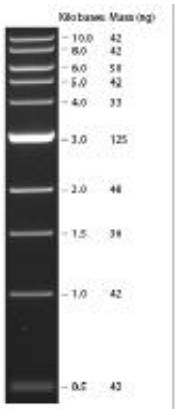

Fragment	Size (bp)	Mass (ng)
1	10,002	42
2	8,001	42
3	6,001	50
4	5,001	42
5	4,001	33
6	**3,001**	**125**
7	2,000	48
8	1,500	36
9	1,000	42
10a	517	42
10b	500	42

SDS Ladder from New England Biolabs

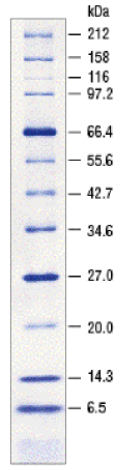

Protein	Source	Molecular Weight (daltons)
Myosin	rabbit muscle	212,000
MBP-β-galactosidase	*E. coli*	158,194
β-Galactosidase	*E. coli*	116,351
Phosphorylase b	rabbit muscle	97,184
Serum albumin	**bovine**	**66,409**
Glutamic dehydrogenase	bovine liver	55,561
MBP2*	*E. coli*	42,710
Thioredoxin reductase	*E. coli*	34,622
Triosephosphate isomerase	***E. coli***	**26,972**
Trypsin inhibitor	soybean	20,100
Lysozyme	chicken egg white	14,313
Aprotinin	bovine lung	6,517
Insulin A	bovine pancreas	3,400
B chain	bovine pancreas	2,340

Concentration: 0.1 mg/ml to 0.2 mg/ml
Recommended Load: 6 µl

NMR Table of position and coupling constanse of different protons

Table 2. ^{1}H and ^{13}C NMR chemical shifts[a] of Nestlé oligosaccharides obtained from curdlan, recorded in D_2O 292K. Coupling constants (Hz) are given between brackets.

Residue	H-1 C-1	H-2 C-2	H-3 C-3	H-4 C-4	H-5 C-5	H-6a C-6	H-6b
DP2							
G1α	5.232 (3.6) 93.1	3.72 72.0	3.91 83.4	3.53 69.2	3.87 72.3	3.85 61.8	3.77
G1β	4.673 (8.5) 96.7	3.44 74.9	3.74 85.7	3.51 69.2	3.49 76.6	3.91 61.8	3.72
$G2_{\alpha}$	4.719 (8.5) 103.9	3.37 74.5	3.54 76.6	3.41 70.6	3.50 76.9	3.92 61.6	3.74
$G2_{\beta}$	4.736 (8.5) 103.9	3.37 74.5	3.54 76.6	3.41 70.6	3.50 76.9	3.92 61.6	3.74
DP3							
G1α	5.232 (3.7) 93.1	3.72 72.0	3.91 83.4	3.53 69.2	3.87 72.3	3.85 61.8	3.77
G1β	4.671 (8.4) 96.7	3.44 74.9	3.74 85.7	3.51 69.2	3.49 76.6	3.91 61.8	3.72
$G2_{\alpha}$	4.758 (8.5) 103.7	3.56 74.3	3.78 85.3	3.53 69.1	3.53 76.7	3.93 61.7	3.74
$G2_{\beta}$	4.776 (8.5) 103.7	3.56 74.3	3.78 85.3	3.53 69.1	3.53 76.7	3.93 61.7	3.74
G3	4.758 (8.5) 103.8	3.36 74.5	3.54 76.6	3.41 70.6	3.49 76.9	3.93 61.7	3.74
DP4							
G1α	5.232 (3.7) 93.1	3.72 72.0	3.91 83.4	3.53 69.2	3.87 72.3	3.85 61.8	3.77
G1β	4.671 (8.5) 96.7	3.44 74.9	3.74 85.7	3.51 69.2	3.49 76.6	3.91 61.8	3.72
$G2_{\alpha}$	4.759 (8.5) 103.7	3.56 74.3	3.78 85.3	3.53 69.1	3.53 76.7	3.93 61.7	3.74
$G2_{\beta}$	4.776 (8.5) 103.7	3.56 74.3	3.78 85.3	3.53 69.1	3.53 76.7	3.93 61.7	3.74
G3	4.800 (8.5) 103.7	3.58 74.3	3.78 85.2	3.53 69.1	3.52 76.6	3.94 61.7	3.74
G4	4.759 (8.5) 103.8	3.36 74.5	3.54 76.6	3.41 70.6	3.49 76.9	3.93 61.7	3.74
DP5-DP10							
G1α	5.232 (3.7) 93.1	3.72 72.0	3.91 83.4	3.53 69.2	3.87 72.3	3.85 61.8	3.77
G1β	4.671 (8.5) 96.7	3.44 74.9	3.74 85.7	3.51 69.2	3.49 76.6	3.91 61.8	3.72
$G2_{\alpha}$	4.759 (8.5) 103.7	3.56 74.3	3.78 85.3	3.53 69.1	3.53 76.7	3.93 61.7	3.74
$G2_{\beta}$	4.776 (8.5) 103.7	3.56 74.3	3.78 85.3	3.53 69.1	3.53 76.7	3.93 61.7	3.74
G3-G9	4.800 (8.5) 103.7	3.58 74.3	3.78 85.2	3.53 69.1	3.52 76.6	3.94 61.7	3.74
G10	4.759 (8.5) 103.8	3.36 74.5	3.54 76.6	3.41 70.6	3.49 76.9	3.93 61.7	3.74

[a]In ppm relative to the signal of internal acetone (δ 2.225 for ^{1}H, δ31.07 for ^{13}C) cortesey of Justina M. Dobruchowska

7. Reference

Anderson, K., Li, S. C., & Li, Y. T. (2000). Diphenylamine-aniline-phosphoric acid reagent, a versatile spray reagent for revealing glyco-conjugates on thin-layer chromatography plates. Analytical Biochemistry, 287(2), 337-9. doi:10.1006/abio.2000.4829

Ausubel, F. M., Brent, R., Kingston, R. E., Moore, D. D., Seidman, J. D., & Smith, J. (Eds.). (2001). Currents Protocols in Molecular Biology (Vols. 1-4, Vol. 3). John Wiley & Sons, Inc.

Bădulescu, M., Apetrei, N. S., Lupu, A., Cremer, L., Szegli, G., Moscovici, M., Mocanu, G., et al. (2009). Curdlan derivatives able to enhance cytostatic drugs activity on tumor cells. Roumanian Archives of Microbiology and Immunology, 68(4), 201-206.

Bhagwat, A. A., Gross, K. C., Tully, R. E., & Keister, D. L. (1996). Beta-glucan synthesis in Bradyrhizobium japonicum: characterization of a new locus (ndvC) influencing beta-(1-->6) linkages. Journal of Bacteriology, 178(15), 4635-4642.

Bhagwat, A. A., Mithöfer, A., Pfeffer, P. E., Kraus, C., Spickers, N., Hotchkiss, A., Ebel, J., et al. (1999). Further studies of the role of cyclic beta-glucans in symbiosis. An NdvC mutant of Bradyrhizobium japonicum synthesizes cyclodecakis-(1-->3)-beta-glucosyl. Plant Physiology, 119(3), 1057-1064.

Bradford, M. M. (1976). A rapid and sensitive method for the quantitation of microgram quantities of protein utilizing the principle of protein-dye binding. Analytical Biochemistry, 72, 248-54.

Bratina, B J, G A Brusseau, and R S Hanson. (1992). Use of 16S rRNA analysis to investigate phylogeny of methylotrophic bacteria. International Journal of Systematic Bacteriology 42, no. 4:645-648.

Breedveld, M. W., & Miller, K. J. (1994). Cyclic beta-glucans of members of the family Rhizobiaceae. Microbiol. Mol. Biol. Rev., 58(2), 145-161.

Chen, R., Bhagwat, A. A., Yaklich, R., & Keister, D. L. (2002). Characterization of ndvD, the third gene involved in the synthesis of cyclic beta-(1 --> 3),(1 --> 6)-D-glucans in Bradyrhizobium japonicum. Canadian Journal of Microbiology, 48(11), 1008-1016.

Chistoserdova, Ludmila, Alla Lapidus, Cliff Han, Lynne Goodwin, Liz Saunders, Tom Brettin, Roxanne Tapia, et al. (2007). Genome of Methylobacillus flagellatus, molecular basis for obligate methylotrophy, and polyphyletic origin of methylotrophy. Journal of Bacteriology 189, no. 11: 4020-4027.

Cogez, V., Talaga, P., Lemoine, J., Bohin, J.-P. (2001). Osmoregulated Periplasmic Glucans of Erwinia chrysanthemi. J. Bacteriol. 183: 3127-3133.Domon, B., & Costello, C. E. (1988). A systematic nomenclature for carbohydrate fragmentations in FAB-MS/MS spectra of glycoconjugates. Glycoconjugate Journal, 5(4), 397-409.

Dai, Kesheng, Guangyu An, and Changgeng Ruan. (2002). Construction and characterization of bispecific single-chain antibody fragments SZ-2/SZ-21 against platelet glycoprotein Ib alpha and beta3. Zhonghua Yi Xue Za Zhi 82(21):1493-7.

Frey, P. A. (1996). The Leloir pathway: a mechanistic imperative for three enzymes to change the stereochemical configuration of a single carbon in galactose. The FASEB Journal: Official Publication of the Federation of American Societies for Experimental Biology, 10(4), 461-70.

Gastebois, A., Mouyna, I., Simenel, C., Clavaud, C., Coddeville, B., Delepierre, M., Latgé, J., et al. (2010). Characterization of a New β(1–3)-Glucan Branching Activity of Aspergillus fumigatus. Journal of Biological Chemistry, 285(4), 2386 -2396.

Goldman, R. C., Sullivan, P. A., Zakula, D. & Capobianco, J. O. (1995). Kinetics of β-1,3 glucan interaction at the donor and acceptor sites of the fungal glucosyltransferase encoded by the BGL2 gene. Eur J Biochem 227, 372–378.

Hartland, R. P., Emerson, G. W., and Sullivan, P. A. (1991). A Secreted β-glucan-branching Enzyme from Candida albicans. Proc. Soc. R. Lond. 246:155-160

Hartland, R.P., Fontaine, T., Debeaupuis, J-P., Simenel, C., Delepierre, M. and Latge, J-P. (1996). A Novel β-(1–3)-Glucanosyltransferase from the Cell Wall of Aspergillus fumigatus Jour.Biol.Chem. 271: 26843–26849.

Hochstenbach, F., Klis, F. M., van den Ende, H., van Donselaar, E., Peters, P. J., & Klausner, R. D. (1998). Identification of a putative alpha-glucan synthase essential for cell wall construction and morphogenesis in fission yeast. Proceedings of the National Academy of Sciences of the United States of America, 95(16), 9161-6.

Holden, H. M., Rayment, I., & Thoden, J. B. (2003). Structure and function of enzymes of the Leloir pathway for galactose metabolism. The Journal of Biological Chemistry, 278(45), 43885-8.

Hreggvidsson, G. O., Jonsson, J. O., Fridjonsson, O. H., Aevarsson, A., Dobruchowska, J., Kamerling, H., Redgwell, R., Hansen, Carl-Eric., and Debeche-Boukhit, T. (2010). Novel non-Leloir beta-glucoisyltransferases from proteobacteria. in press

Jin, Y., Zhang, H., Yin, Y., & Nishinari, K. (2006). Comparison of curdlan and its carboxymethylated derivative by means of Rheology, DSC, and AFM. Carbohydrate Research, 341(1), 90-9

Kim, Y., Kim, E., Cheong, C., Williams, D. L., Kim, C., & Lim, S. (2000). Structural characterization of [beta]--(1-->3, 1-->6)-linked glucans using NMR spectroscopy. Carbohydrate Research, 328(3), 331-341.

Laemmli, U. K. (1970). Cleavage of Structural Proteins during the Assembly of the Head of Bacteriophage T4. Nature, 227(5259), 680-685.

Lequette, Y., Rollet, e., Delangle, A., Greenberg, E.P. annd Bohin, J.P. (2007). Linear osmoregulated periplasmic glucans are encodedby opgGH locus of Pseudomonas aeruginosa. Microbiol. 153: 3255-3263.

Liu, X., Wang, E., Li, Y., & Chen, W. (2007). Diverse bacteria isolated from root nodules of Trifolium , Crotalaria and Mimosa grown in the subtropical regions of China. Archives of Microbiology, 188(1), 1-14.

Maeda, M., & Nishizawa, K. (1968). Fine structure of laminaran of Eisenia bicyclis. Journal of Biochemistry, 63(2), 199-206.

Mah, T. F., Pitts, B., Pellock, B., Walker, G. C., Stewart, P. S. & O'Toole, G. A. (2003). A genetic basis for Pseudomonas aeruginosa biofilm antibiotic resistance. Nature 426, 306–310

McIntosh, M., Stone, B. A., & Stanisich, V. A. (2005). Curdlan and other bacterial (1-->3)-beta-D-glucans. Applied Microbiology and Biotechnology, 68(2), 163-73.

Merry, T. (1999). Current techniques in protein glycosylation analysis. A guide to their application. Acta Biochimica Polonica, 46(2), 303-14.

Mitchell, Terence N., and Burkhard Costisella. 2007. NMR--from spectra to structures: an experimental approach. Springer, September 10.

Mossessova, E., & Lima, C. D. (2000). Ulp1-SUMO crystal structure and genetic analysis reveal conserved interactions and a regulatory element essential for cell growth in yeast. Molecular Cell, 5(5), 865-876.

Motejadded, H., & Altenbuchner, J. (2009). Construction of a dual-tag system for gene expression, protein affinity purification and fusion protein processing. Biotechnology Letters.

Mukhopadhyay, P., Williams, J. & Mills, D. (1988). Molecular analysis of a pathogenicity locus in Pseudomonas syringae pv. syringae. J Bacteriol 170, 5479–5488.

Nakata, M., Kawaguchi, T., Kodama, Y., & Konno, A. (1998). Characterization of curdlan in aqueous sodium hydroxide. Polymer, 39(6), 1475-1481(7).

Pryor, K. D., & Leiting, B. (1997). High-level expression of soluble protein in Escherichia coli using a His6-tag and maltose-binding-protein double-affinity fusion system. Protein Expression and Purification, 10(3), 309-19.

Reis, A., Coimbra, M. A., Domingues, P., Ferrer-Correia, A. J., & Domingues, M. R. M. (2004). Fragmentation pattern of underivatised xylo-oligosaccharides and their alditol derivatives by electrospray tandem mass spectrometry. Carbohydrate Polymers, 55(4), 401-409.

Sadovskaya, Irina, Evgeny Vinogradov, Jianjun Li, Abderrahman Hachani, Karolina Kowalska, and Alain Filloux. (2010). High-level antibiotic resistance in Pseudomonas aeruginosa biofilm: the ndvB gene is involved in the production of highly glycerol-phosphorylated beta-(1->3)-glucans, which bind aminoglycosides. Glycobiology 20, no. 7 (July): 895-904.

Sambrook, J., Frithsch, E. F., & Maniatis, T. (1989). Molecular Cloning. Cold Springs Harbor Labor Press, New York.

Spicer, E. J., Goldenthal, E. I., & Ikeda, T. (1999). A toxicological assessment of curdlan. Food and Chemical Toxicology: An International Journal Published for the British Industrial Biological Research Association, 37(4), 455-79.

Stasinopoulos, S. J., Fisher, P. R., Stone, B. A., & Stanisich, V. A. (1999). Detection of two loci involved in (1-->3)-beta-glucan (curdlan) biosynthesis by Agrobacterium sp. ATCC31749, and comparative sequence analysis of the putative curdlan synthase gene. Glycobiology, 9(1), 31-41.

Steinbüchel, E. A., & Rhee, S. K. (2005). Polysaccharides and Polyamides in the Food Industry. Wiley-VCH Verlag

Talaga, P., Fournet, B. & Bohin, J.-P. (1994). Periplasmic glucans of Pseudomonas syringae pv. syringae. J Bacteriol 176, 6538–6544.

Terpe, K. (2003). Overview of tag protein fusions: from molecular and biochemical fundamentals to commercial systems. Applied Microbiology and Biotechnology, 60(5), 523-533.

Wong, C., Sridhara, S., Bardwell, J. C., & Jakob, U. (2000). Heating greatly speeds Coomassie blue staining and destaining. BioTechniques, 28(3), 426-428, 430, 432.

Zubrick, J. W. (1997) The Organic Chem Lab Survival Manual. John Wiley & Sons, Inc. Fourth edition